Accumulated Creep Strain and Energy Density Based Thermal Fatigue Life Prediction Models for SnAgCu Solder Joints

Ahmer Syed
Amkor Technology, Inc.
1900 S. Price Road
Chandler, AZ 85248
asyed@amkor.com

Abstract

Pb free solder is fast becoming a reality in electronic manufacturing due to marketing and legislative pressures. The industry has pretty much concluded that various version of SnAgCu solder alloy offer the best alternative for eutectic Sn/Pb solder currently in use. With the current trend of cheaper, faster, and better electronic equipment, it has become increasingly important to evaluate the package and system performance very early in the design cycle using simulation tools. This requires life prediction models for new solder alloy systems so that the package-to-board interconnect reliability can be predicted for various environmental and field conditions.

This paper describes in detail the life prediction models for SnAgCu solder joints. The models are based on published constitutive equations for this alloy and thermal cycle fatigue data on actual components. The approach uses advance finite element modeling and analysis techniques and is based on mechanics of deformation. Both accumulated creep strain and creep strain energy density based models are developed. The model has been correlated with a number of data points and predicts life within 25% in most cases. The framework of modeling and prediction methodology described here is fully compatible with the framework used for SnPb solder previously.

Introduction

The reliability of solder joints is one of the most important factors when selecting a package for a particular application. The CTE and stiffness mismatch between the package and the board results in thermal stresses in solder joints during temperature and power cycling. The damage caused by these stresses accumulates as the electronic assembly is subjected to multiple cycles, ultimately causing failures of solder joints. This is a very well documented failure mode for electronic assemblies and a wealth of data is available in the literature for SnPb solder. Due to this reason, the reliability of Pb free solder joints is an important factor for selecting the proper replacement of SnPb solder. Based on various studied conducted, the industry as a whole has converged towards SnAgCu solder alloy (with different compositions) to replace SnPb solder from electronic assemblies.

The reliability of SnAgCu solder joints has been a subject of major research in electronic industry and a number of researchers have published data [1, 2, 3] showing SnAgCu performs better or worse than SnPb solder, depending on the components tested and test conditions employed. While more test data is being gathered under accelerated test conditions, it is also becoming apparent that this will not be enough due to rapid implementation of this soldering system. Today, electronic industry uses electronic components using lead frame or laminate technology with countless number of packages in various lead counts, lead/ball pitches, and die sizes. Since every component has a different interconnect reliability behavior, it is unrealistic and cost prohibitive to generate test data for every case. The interconnect reliability also depends on other factors such as the motherboard thickness and actual end use application and data generated on one test condition may not be useful for all. With the current trend of cheaper, faster, and better electronic equipment, it has become increasingly important to evaluate the package and system performance for its intended application very early in the design cycle using simulation tools. The life prediction of solder joints is an important part of this evaluation and models are needed to virtually qualify a package without extensive test data. This requires a life prediction model, which is based on damage mechanisms and can predict life accurately.

Developing a life prediction model for solder joints requires four main ingredients and all of these contribute significantly to the accuracy of life prediction model:

- Constitutive equation and material properties for the applicable range of stress conditions,
- A damage mechanism based methodology based on constitutive behavior of the material,
- Actual test data on real components including failure mechanism, and
- Simulation to calculate the response of solder joint under different stress conditions.

Using the above four ingredients, the author has proposed a life prediction model for SnPb solder joints previously [4, 5]. This model has been validated with more than 75 data points and predicts life within 25% in most cases. This proven approach is used here again to develop the life prediction model for SnAgCu solder joints.

Actual test data on various packages is generated and the same package attributes and test conditions are simulated using published constitutive equations for SnAgCu solder. The solder joint response (partitioned creep strain, total creep strain, and creep strain energy density) are then used to determine the parameters of damage mechanism based life prediction models. The life prediction models reported here are only applicable for thermal and power cycle fatigue, where the

A Note to reader: This paper was originally published in ECTC 2004 conference proceedings (pp 737 – 746), however, due to errors in data processing the constants for life prediction models published in the original paper were not accurate. These constants, along with associated figures, have been corrected here.

cycling conditions are quite different from a fast cycle bending or vibration fatigue.

Constitutive Models for SnAgCu solder

The melting point of SnAgCu (Ag: 3.0 – 4.0%, Cu: 0.5 to 1.0%) is typically observed as 217°C. This means that the homologous temperature (the ratio of operating and melting temperature in absolute scale) is about 0.47 at –40°C. It is well documented that creep plays a very important role in deformation behavior of materials at homologous temperatures close to and above 0.5 if the loading rate is slow enough for creep deformations to occur. Since in actual use conditions, the temperature cycle duration is in the order of minutes to days and the homologous temperature is more than 0.5, solder joints formed by using SnAgCu solder alloy are expected to deform primarily due to creep.

Recently, a number of papers have been published [6, 7, 8, 9] on the constitutive equation for creep deformation for SnAgCu alloy for compositions currently in considerations. Wiese et al [6] studied the creep behavior of bulk, PCB sample, and Flip Chip solder joint samples of Sn4.0Ag0.5Cu solder and identified two mechanisms for steady state creep deformation for the bulk and PCB samples. They attributed these to climb controlled (low stress) and combined glide/climb (high stress) behavior and represented steady state creep behavior using double power law model.

Schubert et al [7] combined data from different sources and from their own testing on different compositions of SnAgCu solder (Sn3.8Ag0.7Cu, Sn3.5Ag0.75Cu, Sn3.5Ag0.5Cu, and Castin™). They also identified two regions for stress-strain rate behavior, but postulated the high stress region as power law break-down region, and chose hyperbolic sine function to represent creep data.

Zhang et al [8] generated their data on single lap shear specimen of Sn3.9Ag0.6Cu solder alloy. The also modeled the steady state creep behavior using hyperbolic sine function postulating power law break-down at high values of stress. Finally, Morris et al [9] used double power law constitutive model to represent creep data on single lap shear specimens of Sn3.0Ag0.5Cu solder joints. The stress exponents of 6.6 and 10.7 were suggested for the low and high stress regions.

The above constitutive equations and their respective parameters, converted to tensile stress-strain rate format, are shown in Table 1. The reported modulus, CTE, and Poisson's ratio values are also included for the respective model, wherever provided. It should be noted that while steady state creep deformation is usually attributed to distinct regions - and different regions have been suggested for creep deformation of SnAgCu by different researchers - these regions are identified as "Mechanism 1" and "Mechanism 2" in the following to avoid multiple subscripts.

The above constitutive models as well as measured data from [9, 10] are plotted in Figure 1 for three different temperatures and are compared with published constitutive model of SnPb solder [11]. The figure clearly shows that the predicted steady state creep rate for SnAgCu solder is two to four orders of magnitude lower than that for SnPb solder for the same temperature at low stress levels. As the stress increases, all models for SnAgCu show steeper slope of strain rate vs. stress curve compared to SnPb solder with different cross-over points depending on the constitutive model and the temperature. This means that except for very high stress values, .SnAgCu is generally more creep resistant than SnPb solder. This partly explains why solder joints made with this particular solder tend to last longer in temperature cycle tests except for the stiffer assemblies which result in higher stresses [1, 2, 3].

Table 1: Constitutive Relations for SnAgCu Solder

Reference	Constitutive Model
Wiese et al [6] **Equation : 1**	$\dot{e}_{cr} = A_1 \exp\left(\frac{-H_1}{kT}\right)\left(\frac{s}{s_n}\right)^{n_1} + A_2 \exp\left(\frac{-H_2}{kT}\right)\left(\frac{s}{s_n}\right)^{n_2}$ A_1 = 4E-7 s^{-1}, H_1/k = 3223, n_1 = 3.0, A_2 = 1E-12 s^{-1}, H_2/k = 7348, n_2 = 12, σ_n = 1 MPa E(MPa) = 59533 – 66.667T(°K)
Schubert et al [7] **Equation : 2**	$\dot{e}_{cr} = A_1[\sinh(a\,s)]^n \exp\left(\frac{-H_1}{kT}\right)$ A_1 = 277984 s^{-1}, a = 0.02447 MPa^{-1}, n = 6.41, H_1/k = 6500 E(MPa) = 61251 – 58.5T(°K) , CTE = 20.0 ppm/K, Poisson's ratio = 0.36
Zhang et al [8] Converted to tensile form	$\dot{e}_{cr} = A_1[\sinh(a\,s)]^n \exp\left(\frac{-H_1}{kT}\right)$ A_1 = 143.4 s-1, a = 0.108 MPa^{-1}, n = 3.7884, H_1/k = 7567 E(MPa) = 24224 – 0.0206(°K)
Morris et al [9]	Double power law: H_1/k = 11425, n_1 = 6.6, H_2/k = 9020, n_2 = 10.7 G(MPa) = 27360 – 40.5T(°K)

Comparing the creep curves for SnAgCu from different constitutive models, the steady state creep behavior for this alloy seems to be bounded is a narrow band even though there are differences between samples preparation, test methods, and alloy composition. It should be noted that all plots in Figure 1, except for data from [10], are based on constitutive models, which are themselves fitted from actual data. The plots show that constitutive model proposed by Schubert et al [7] and Zhang et al [8] predict very similar behavior at low stresses but start diverging at higher stresses (around 30 MPa). On the other hand, the model proposed by Wiese et al [6], predicts lower creep rate at low stresses (below 30 MPa) but higher rate than Schubert's model at high stresses.

A Note to reader: This paper was originally published in ECTC 2004 conference proceedings (pp 737 – 746), however, due to errors in data processing the constants for life prediction models published in the original paper were not accurate. These constants, along with associated figures, have been corrected here.

The actual data from [10], however, shows different behavior depending on the temperature. It correlates better with Wiese's model at lower temperatures but falls close to Schubert's and Zhang's model at high temperatures. This difference can be attributed to significantly different alloy composition for this data (Sn3.0Ag0.5Cu) compared to the other data generated on higher Ag percentage.

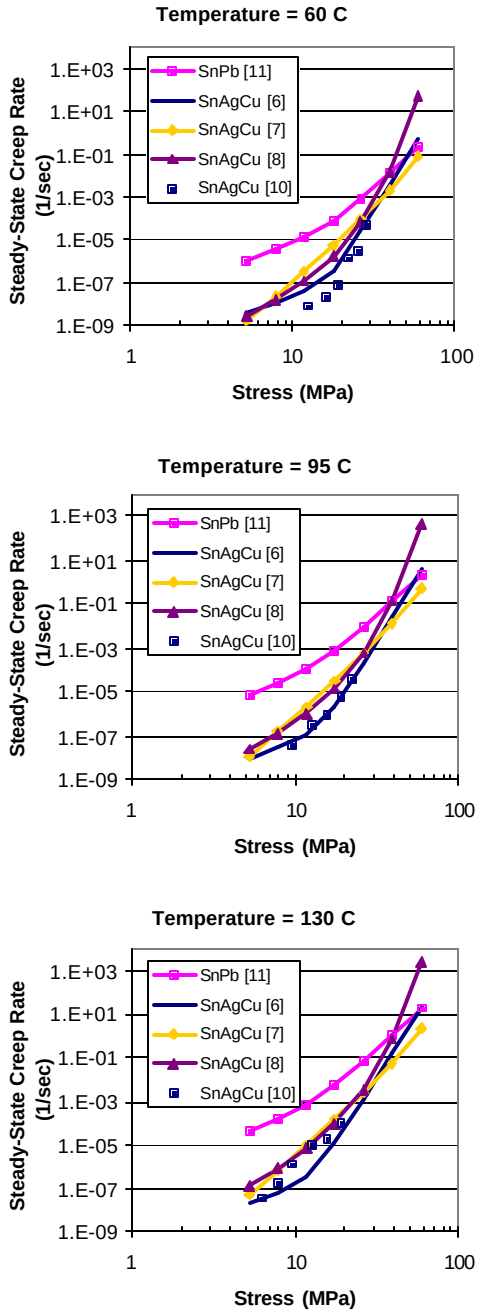

Figure 1: Comparison of Creep Models for SnAgCu.

Because of narrow band in data scatter, any of these constitutive models can be employed to simulate the deformation behavior of SnAgCu solder joints. However, the models given by Equation 1 and 2 in Table 1 are selected here as the solder composition is closer to one used to generate the test data and because of similar modulus values reported. A more detailed comparison of life prediction models using various constitutive models will be presented elsewhere.

Life Prediction Methodology

A number of life prediction models have been proposed in the literature for SnPb solder [5, 12, 13] and more recently for SnAgCu solder interconnects [7, 8]. These models are either based on strain range, accumulated creep strain, or accumulated strain energy density during a temperature cycle. The author has previously proposed a partitioned accumulated creep strain model for SnPb solder [4, 5] based on damage mechanisms as described by the constitutive equation. The basic assumption for this life prediction model is that the damage in solder joint during temperature cycling is primarily due to steady state creep strain accumulation. Although the primary creep and time independent plasticity may play a role also, it is assumed that these effects are minor and can be included in a strain rate model as has been done by Darveaux et al [12]. Since creep is considered as the primary damage mechanism for SnAgCu solder during thermal cycling and is solely used here to simulate the material behavior, the theoretical basis for the life prediction model has to be creep deformation also. Specifically, instead of using the traditional definition of fatigue, the cyclic loading is considered as a special case of creep due to sequence of loading which are repeated in a cyclic manner to derive the life prediction model parameters. This is done by using two equations; a) Monkmann-Grant equation for creep rupture, and b) time-fraction rule.

The Monkmann-Grant equation for creep rupture, as given in Equation 3, states that the time to rupture, t_r, is inversely related to the steady state creep strain rate, $\dot{e}_{cr}$, during a test.

$$t_r = \frac{e_f}{\dot{e}_{cr}} \tag{3}$$

The constant e_f gives the "creep ductility" or the strain at the onset of failure. The above equation assumes a constant stress during the creep test.

In case of varying stresses repeated in a cyclic manner, an estimate of rupture time (or cycles to failure) can be made by using a special form of time-fraction rule, as given by Equation 4. Notice the similarity of term within the summation sign to the more familiar Palmgren-Miner rule for cyclic damage.

$$N_f \left(\sum_{i=1}^{n} \frac{\Delta t_i}{t_{ri}} \right) = 1 \tag{4}$$

where,

N_f = number of repetitions or cycles to failure,
n = number of steps within a cycle,
Dt_i = time spent at stress level s_i within a cycle, and
t_{ri} = rupture time for stress level s_i.

Using Monkmann-Grant equality, Equation 4 becomes

A Note to reader: This paper was originally published in ECTC 2004 conference proceedings (pp 737 – 746), however, due to errors in data processing the constants for life prediction models published in the original paper were not accurate. These constants, along with associated figures, have been corrected here.

$$N_f \left(\frac{\sum_{i=1}^{n} \Delta t_i \ \dot{e}_{cri}}{e_f} \right) = 1 \qquad (5)$$

Where $\dot{e}_{cri}$ is the steady state creep rate for stress level s_i. Realizing that the numerator term within the summation sign is the creep strain accumulated during time Dt_i, the summation for all steps n within a cycle gives the Accumulated Creep Strain, ε_{acc} , for the whole cycle. Thus, the above Equation can be simplified as

$$N_f = (C' e_{acc})^{-1} \qquad (6)$$

where,

N_f = number of repetitions or cycles to failure,

e_{acc} = Accumulated creep strain per cycle,

C' = $1/e_f$, inverse of creep ductility.

Notice that the strain exponent is -1 for this life prediction model.

Equation 6 can also be derived using a fracture mechanics approach, as discussed previously [14]. It has also been shown by the author [14] that this equation can easily be converted into energy density based life prediction model:

$$N_f = (W' w_{acc})^{-1} \qquad (7)$$

where,

N_f = Number of repetitions or cycles to failure,

w_{acc} = Accumulated creep energy density per cycle,

W' = Creep energy density for failure.

Equations 6 and 7 give the cyclic creep ("Fatigue") life due to varying and repeated stresses for a single creep mechanism. For two creep mechanisms, such as Equation 1 in Table 1 for SnAgCu solder, the above equations become

$$N_f = \left(C_I \, e_{acc}^{I} + C_{II} \, e_{acc}^{II} \right)^{-1} \qquad (8)$$

and

$$N_f = \left(W_I \, w_{acc}^{I} + W_{II} \, w_{acc}^{II} \right)^{-1} \qquad (9)$$

The above life prediction models require the determination of constants C', C_I and C_{II} for creep strain based model and W', W_I , and W_{II} for dissipated creep energy density based model, depending on the number of damage mechanisms used accumulated creep strain or creep strain energy density calculated simulating the same test conditions.

For eutectic SnPb solder the constants in equations 8 & 9 have been determined by the author [14] and the proposed life prediction models are given by:

$$N_f = \left(0.02 e_{acc}^{I} + 0.063 e_{acc}^{II} \right)^{-1} \qquad (10)$$

$$N_f = \left(0.0027 \, w_{acc}^{I} + 0.0019 \, w_{acc}^{II} \right)^{-1} \qquad (11)$$

The above models were originally developed with a limited set of data points [14] but have since been validated with more than 75 data points.

A similar approach is attempted here for SnAgCu solder using the constitutive equations given by Equations 1 and 2. The constitutive model from Equation 1 is a double power law model and creep strain and energy density can be partitioned into their respective mechanisms. On the other hand, the constitutive model in Equation 2 does not separate the two damage mechanisms and partitioning of creep strain or energy density is not attempted.

The determination of life prediction model parameters requires actual test data measuring the cycles to failure during temperature cycle tests (N_f), and some way of quantifying the strain or strain energy density during the temperature cycle. In the following sections the test data is first described followed by simulation methodology to calculate solder joint response.

Solder Joint Reliability Test Data

In order to evaluate the reliability of solder joints, accelerated temperature cycle tests were conducted on various packages comparing the reliability of SnAgCu solder with that of SnPb eutectic solder. Table 2a lists the test data points used here for life prediction model development. The data was generated on packages of sizes varying from 8x8 mm to 27 x 27mm and various die sizes. The packages were constructed of three substrate materials, four ball pitches, and four ball sizes to cover the range of BGAs and CSPs.

The daisy chained packages were assembled using either SnAgCu (4.0Ag0.5Cu or 3.9Ag0.5Cu) or SnPb balls and were mounted on test boards using SnAgCu or SnPb paste, respectively. The test boards of various thickness' had alternate daisy chains so one or more nets were formed after package assembly on board. All packages used in this comparison used electrolytic NiAu plating on the ball lands and the test boards had OSP surface finish.

The assembled boards were placed inside thermal cycle chambers and cycled according to prescribed condition. Three test conditions were used to generate this data:

- TC1: -40 to 125°C temp cycle, 15 minutes ramps and dwells, 1 cycle per hour,
- TC2: -55 to 125°C, 12 minutes ramps and 3 minutes dwells, 2 cycles/hour, and
- TC3: 0 to 100°C, 10 minutes ramps and 5 minutes dwells, 2 cycles/hour.

These temperature cycle conditions cover the range of accelerated conditions typically used by the industry to evaluate solder joint reliability for various applications. The temperature profiles mentioned above were measured at the test boards during the cycling and are not the chamber profiles. The testing also employed in-situ resistance measurement to detect failures. The resistance of each electrical net was measured every two minutes and was compared with the threshold resistance of 300 ohms. A net is considered as failed at the first instance when its resistance exceeded the threshold value followed by ten additional such instances within 10% of the time of first failure. The failures

A Note to reader: This paper was originally published in ECTC 2004 conference proceedings (pp 737 – 746), however, due to errors in data processing the constants for life prediction models published in the original paper were not accurate. These constants, along with associated figures, have been corrected here.

were also confirmed manually within a week of first occurrence. The failure data was further analyzed by Weibull analysis software to determine Weibull parameters (slope β and characteristic life ε) and the mean life. Note that the mean life is not the characteristic life and is calculated from β and ε parameter using Gamma function.

Table 2a: Package and test condition for board level reliability tests

Data Point	Package Type	Substrate Type	Body Size	I/O	Pitch	Die Size	Pad Type	Pad Size	Ball Dia	Test Type	Board Thickness
1	CABGA	Laminate	15 x 15	208	0.8	8.5 x 8.5 x0.265	SMD	0.4	0.46	TC1	1.0
2	CABGA	Laminate	15 x 15	256	0.65	10 x 10 x 0.265	SMD	0.32	0.4	TC2	0.8
3	CABGA	Laminate	8 x8	64	0.8	4.8 x 4.8 x 0.29	SMD	0.4	0.46	TC1	1.6
4	CABGA	Laminate	8 x8	64	0.8	4.8 x 4.8 x 0.29	SMD	0.4	0.46	TC2	1.6
5	Ceramic BGA	Ceramic	8 x8	64	0.8	None	SMD	0.4	0.46	TC1	1.6
6	Ceramic BGA	Ceramic	8 x8	64	0.8	None	SMD	0.4	0.46	TC3	1.6
7	CVBGA	Laminate	12 x 12	288	0.5	7.1 x 7.1 x 0.175	SMD	0.25	0.3	TC1	0.8
8	fleXBGA	Tape	12 x 12	144	0.8	6.4 x 6.4 x 0.3	SMD	0.3	0.46	TC1	1.6
9	fleXBGA	Tape	12 x 12	144	0.8	6.4 x 6.4 x 0.3	SMD	0.3	0.46	TC2	1.6
10	fleXBGA	Tape	12 x 12	144	0.8	6.4 x 6.4 x 0.3	SMD	0.3	0.46	TC3	1.6
11	PBGA	Laminate	27 x 27	256	1.27	10 x 10 x 0.30	SMD	0.65	0.76	TC2	1.6
12	TSCSP	Tape	12 x 12	288	0.5	top: 5.08 x 5.08 x 0.15, btm: 10.16 x 10.16 x 0.15	SMD	0.24	0.3	TC2	0.8

Table 2b: Board level reliability test results for SnAgCu and SnPb solder joints

				SnAgCu Solder				SnPb Eutectic Solder			
Data Point	Package Type	Body Size	I/O	1st Failure	Weibull Slope	Weibull Char. Life (Cycles)	Mean Life (Cycles)	1st Failure	Weibull Slope	Weibull Char. Life (Cycles)	Mean Life (Cycles)
1	CABGA	15 x 15	208	2491	8.92	3717	3520	2539	10	3450	3281
2	CABGA	15 x 15	256	3380	15.4	4096	3960	1856	7.4	2725	2557
3	CABGA	8 x8	64	3463	8.36	4843	4570	2445	11.76	3212	3076
4	CABGA	8 x8	64	2493	9.81	3263	3103	2205	13.76	2664	2565
5	Ceramic BGA	8 x8	64	318	7.08	445	417	340	10	437	416
6	Ceramic BGA	8 x8	64	853	9.55	1103	1047	982	8.96	1316	1246
7	CVBGA	12 x 12	288	1332	5.81	2005	1890	1700	9.26	2291	2172
8	fleXBGA	12 x 12	144	2580	19.06	2948	2868	2369	10.4	3164	3015
9	fleXBGA	12 x 12	144	2351	20.4	2792	2720	1902	15.2	2410	2327
10	fleXBGA	12 x 12	144	8939	15.7	10370	10027	5042	12.95	6195	5953
11	PBGA	27 x 27	256	4651	7.2	6812	6381	3656	13.92	4544	4378
12	TSCSP	12 x 12	288	175	6	296	275	NA	NA	NA	NA

Table 2b lists the Weibull parameters and the mean life for both SnPb and SnAgCu solder joints for each data point. The data shows that while SnAgCu solder joints had a higher reliability for most cases SnPb solder joints lasted longer in some cases. The measured mean life covers a range of data from 275 cycles to 10027 cycles for SnAgCu and 416 to 5953 cycles for SnPb solder joints, respectively.

In all cases reported here, the solder joints failed at package interface. Figure 2 shows a typical cross-section of failed joint showing crack very close to intermetallic on package side.

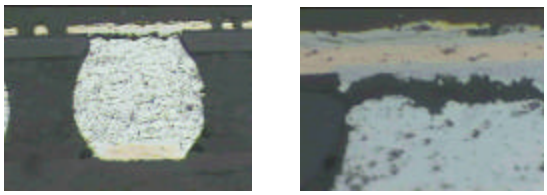

Figure 2: Typical failed SnAgCu solder joint cross-section.

Finite Element Simulations

The above test data points were simulated in finite element analysis using ANSYS™ to calculate the accumulated creep strain or energy density during each temperature cycle. The details of the simulation approach have been described elsewhere [5] and are not repeated here. Briefly, the modeling approach involves a global-local method where a 3-D global model ($1/4^{th}$ or $1/8^{th}$ symmetric) model is generated in the first step using SOLID185 elements in ANSYS, encompassing all geometric details of the package-board assembly and linear material properties. The model is analyzed for a unit temperature drop using sub-structuring analysis methods. The super-element so generated is then used in a detailed model of the critical solder joint using SOLID185 elements. This detailed solder joint model includes the geometric shape of the joint as well as intermetallics and interfacing package and board pads. The super-element is also added to this model to get the effect of package stiffness. The solder material is modeled using creep and temperature dependent properties. The model is then analyzed for one or two complete temperature cycles, simulating the actual profile as much as possible. The output from this simulation includes the accumulated creep strain and dissipated creep strain energy density (ANSYS Output parameters: NL, CREQ and SEND, CREEP). A volume averaging technique is then employed to calculate the accumulated creep strain or energy density for 25 micron thick

A Note to reader: This paper was originally published in ECTC 2004 conference proceedings (pp 737 – 746), however, due to errors in data processing the constants for life prediction models published in the original paper were not accurate. These constants, along with associated figures, have been corrected here.

layers of solder at package and board interface, respectively. These layers contain two elements across the thickness to mitigate any stress singularity issues [14]. Figure 3 shows a sample finite element model for package and solder joint.

This modeling approach has been successfully used for SnPb solder and is applied for SnAgCu solder joints as well. It should be noted here that although advanced finite element analysis techniques are used here, they are primarily to enhance the efficiency of analysis. It is not required that the simulation approach be implemented as is to use the life prediction model. The only requirements are: 3-D modeling ($1/4^{th}$ or $1/8^{th}$ symmetric), and volume averaging on a 25 micron thick layer of solder at interfaces, each with at least two elements across the thickness.

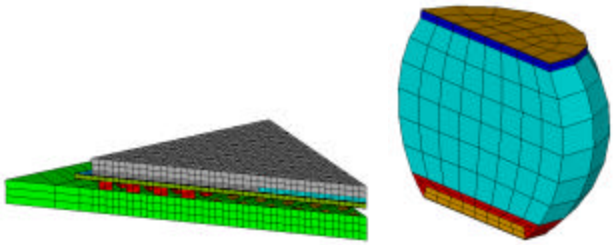

Figure 3: Global finite element model and detailed solder joint model. Blue and red elements in solder joint model indicate 25 micron thick solder layers at package and board interface, respectively.

Life Prediction for SnPb Solder Joints

The test data described above contains measured mean life for both SnPb and SnAgCu solder joints. In order to revalidate the earlier published model for SnPb solder, the 11 data points for SnPb solder were simulated first in finite element using above methodology to predict the life.

For SnPb solder, the following constitutive equation [11] is used to simulate the creep behavior

$$\dot{e}_{cr} = B_I \exp\left(\frac{-H}{kT}\right)\left(\frac{s}{\mathrm{E}(T)}\right)^{n_1} + B_{II} \exp\left(\frac{-H}{kT}\right)\left(\frac{s}{\mathrm{E}(T)}\right)^{n_2} \quad (12)$$

Steady State Creep Model Parameters (SnPb)				
B_I	B_{II}	H	n_1	n_2
1.7e12 1/sec	8.9e24 1/sec	0.468 eV	3	7

With E (T) = -0.088T(^{o}C) + 32 GPa.

The life prediction models are given by Equation 10 & 11.

Figure 4 shows the comparison of measured and predicted mean life. The predicted life for these new data points is again within 25% of measured life and provides further validation of the life prediction model. The good correlation between predicted and measured fatigue life for SnPb solder also indicates that the material properties used for other materials (mold compound, die attach, substrate, test board, etc) are accurate. The property values used here for mold compound and die attach materials are based on DMA and TMA data generated at Amkor's lab and not from supplier's provided data sheets.

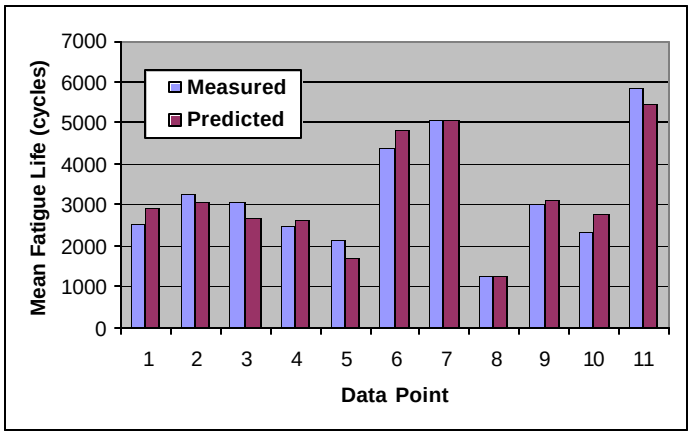

Figure 4: Comparison of predicted and measured mean life for eutectic SnPb solder joints.

Life Prediction for SnAgCu solder Joints for Double Power Law Creep Model

Having established the confidence in material and geometric parameters of the finite element models for packages with SnPb solder joints, the same models were analyzed again but with SnAgCu constitutive model and material properties. Thus any differences between solder joint response (strain and energy density) for the two solder alloys (SnPb and SnAgCu) were only due to the difference in constitutive models and material properties of solder alloy itself. The constitutive model and elastic modulus given by Equation 1 & 2 in Table 1 are used here to simulate solder joint behavior during temperature cycling. The CTE and Poisson's ratio for SnAgCu solder were assumed as 20 ppm/oC and 0.36, respectively as per [7]. The simulated results for each data point were post-processed to calculate the volume averaged accumulated creep strain and creep strain energy density per cycle. In addition, since Equation 1 is of double power law form, accumulated creep strain was also partitioned into its respective mechanism to determine if a life prediction model based on partitioned creep strain, similar to the one used for SnPb solder, can be established. This resulted in three life prediction models, one each for partitioned accumulated creep strain, total accumulated creep strain, and creep strain energy density. The following sections discuss each of these life prediction models. In all cases reported here, the failure was observed and predicted at the package interface.

Partitioned Accumulated Creep Strain: The constitutive model for SnAgCu solder given by Equation 1 describes two mechanisms of creep deformation. It can be argued that each of these mechanisms will cause its own damage and the fatigue life of solder joint should be a function of damage from each mechanism, as given by equations 8 and 9 above.

The creep strain partitioning approach requires the separation of total accumulated creep strain into its respective

A Note to reader: This paper was originally published in ECTC 2004 conference proceedings (pp 737 – 746), however, due to errors in data processing the constants for life prediction models published in the original paper were not accurate. These constants, along with associated figures, have been corrected here.

components. Since ANSYS does not provide separate values for each component, post-processing routine was used to separate the total creep strain into its components. The creep equation was implemented using ANSYS standard implicit creep model (TBOPT = 11). Notice that User Subroutine is no longer required for ANSYS 7.0 to partition the creep strain and higher as was done for SnPb solder in the approach described in [5].

In order to determine the constants of life prediction model, Equation 7, linear multiple regression analysis was performed on two extremes and a few intermediate data points (measured mean life) along with the corresponding partitioned accumulated creep strains. The constants were determined to be 0.106 and 0.045, respectively with a co-efficient of determination of 0.997. Notice that these constants can be taken as the inverse of creep ductility for each mechanism. With these, the life prediction model for SnAgCu is given as:

$$N_f = \left(0.106 e^{I}_{acc} + 0.045 e^{II}_{acc}\right)^{-1} \qquad (13)$$

The above model suggests that SnAgCu is about 2.3X more ductile at higher stress (mechanism II). However, the curve fitting indicated standard error for constants as 0.08 and 0.002, respectively, thus less confidence in the predicted value of 0.106 for C_I . The higher value for standard error for constant C_I indicates significantly higher scatter in the data, as shown in Figure 5.

Figure 6 compares the relative contribution of accumulated creep strain from low stress mechanism for the two alloys for the 11 cases. It is interesting to note that while strain contributions from low stress mechanism are higher for SnPb solder, they are less than 5% on the average for SnAgCu solder. This small contribution of Mechanism I creep strain for SnAgCu solder joint is primarily due to very low creep rates at low stresses. Since the stress changes continuously during the cycle, the total creep strain is dominated by the contributions from higher stress region. Furthermore, since the creep resistance of SnAgCu solder at low stresses is much higher compared to SnPb solder, the solder joints made with this alloy can last a much longer time if the stresses are low.

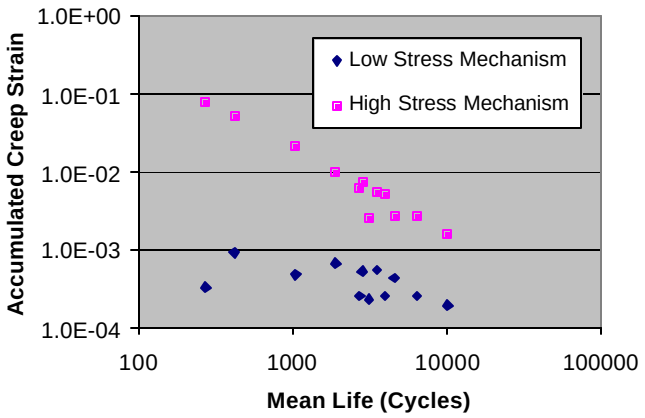

Figure 5: Contribution of each mechanism in total accumulated creep strain vs. measured mean life. Significantly higher scatter in data for low stress mechanism.

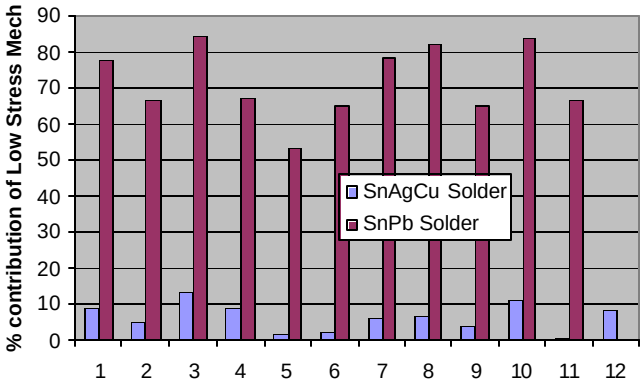

Figure 6: Comparison of relative contribution of low stress mechanism in accumulated creep strain.

Converting the above partitioned creep strains into damage using the life prediction models above, the damage contribution of low stress mechanism for SnAgCu is predicted to be less than 2% on the average. This is in direct contrast to damage contributions from each mechanism for SnPb solder, where the two mechanisms contributed almost the same amount of damage on the average. This indicates that while damage separation is required for SnPb solder, there is no need for such a separation for SnAgCu solder as almost all damage is caused by strain due to higher stress region for this solder. It should be noted, however, that the cases analyzed here are for accelerated test conditions with wide range of temperature change during a cycle. In real applications, the temperature range can be very small during mini cycles and contributions from low stress region can become prominent, requiring damage separation for more accurate life prediction for field cases.

Total Accumulated Creep Strain: Since the damage contribution for low stress region is very small for SnAgCu solder (at least for accelerated test cases), it is possible to use a simplified life prediction model based on total accumulated creep strain. This also simplifies the effort required in simulating the behavior of SnAgCu using ANSYS as there is no need to implement user defined creep law. The standard outputs from ANSYS (NL, CREQ & SEND, CREEP) provide the accumulated creep strain and creep energy density, which can be volume averaged by simple post-processing steps using ETABLES.

In order to determine the total accumulated creep strain (and energy density), the double power law model in Equation 1 was implemented using ANSYS' standard implicit creep equation (TBOPT = 11 with $C_3 = 0$). All 12 data points listed in Table 2 were then simulated. The accumulated creep strains for each element of solder joint were stored in NL, CREQ for every step of the temperature cycle, which were then post-processed

A Note to reader: This paper was originally published in ECTC 2004 conference proceedings (pp 737 – 746), however, due to errors in data processing the constants for life prediction models published in the original paper were not accurate. These constants, along with associated figures, have been corrected here.

to determine the volume averaged accumulated creep strain in the 25 microns thick layer of solder.

The total accumulated strain for the two solder alloys are compared in Figure 7, which shows that the total accumulated creep strain for SnAgCu solder joint can be very similar, higher, or lower than those for SnPb joint for the same package and test condition.

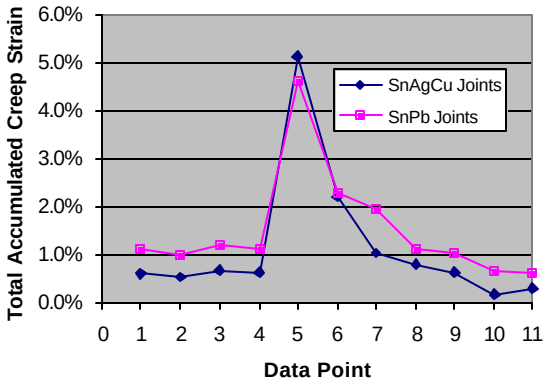

Figure 7: Comparison of accumulated creep strain in SnPb and SnAgCu solder joint.

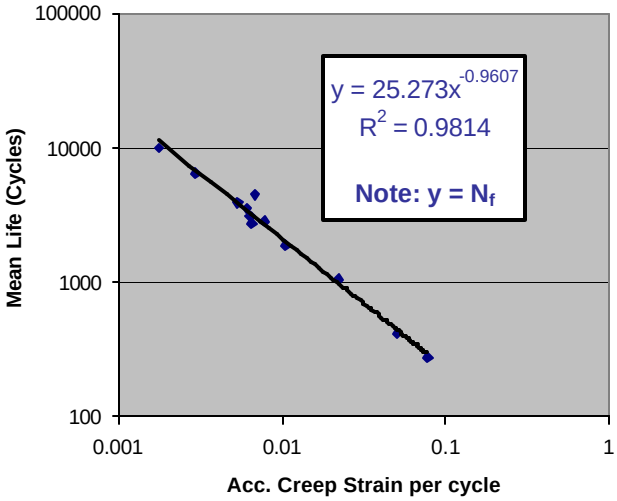

Figure 8: Mean Life vs. Total Accumulated Creep Strain on log-log scale.

Figure 8 shows strain vs. life plot on a log-log scale, the typical format for such representation. Also shown is the fitted model relating mean life with volume averaged accumulated creep strain. Notice that the fitted model predicts the strain exponent as –0.9607, a value very close to the theoretically derived exponent of –1.0 discussed in earlier section. This shows that the fatigue life model given by Equation 6 is valid and data can be fitted with linear regression analysis.

Figure 9 shows the same data replotted on the log-log scale but with strain plotted against the inverse of life. The linear regression analysis with intercept = 0 of this representation shows even a better fit to data, resulting in life prediction model in the same form as Equation 6 with constant C' = 0.0468. The life prediction model for SnAgCu thus becomes

$$N_f = (0.0468\, e_{acc})^{-1} \quad (14)$$

Notice that the constant for total creep strain based model, i.e., 0.0468, is very similar to the constant for Mechanism II of partitioned creep model (0.045). This is because the total accumulated creep strain is only slightly higher than accumulated creep strain due to "Mechanism II".

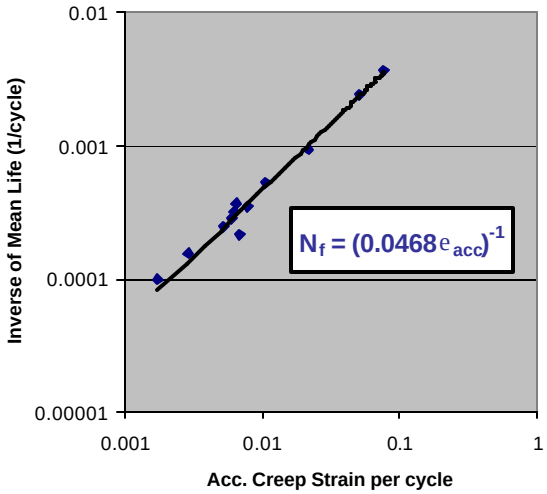

Figure 9: Inverse of Mean Life vs. Total Accumulated Creep Strain on log-log scale.

Creep Strain Energy Density: Plastic or creep strain energy density (sometimes referred as plastic work) has also been used previously to predict the fatigue life of solder joints. Since the finite element simulations can calculate both accumulated creep strain and dissipated creep strain energy density from one analysis, life prediction models for SnAgCu are also determined using Creep Strain Energy Density.

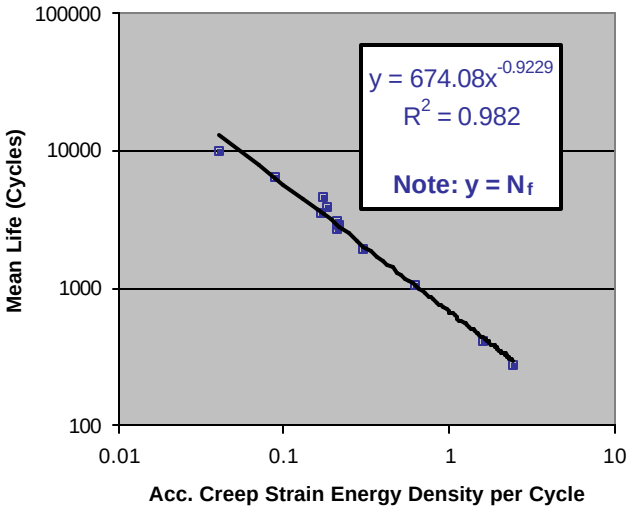

A Note to reader: This paper was originally published in ECTC 2004 conference proceedings (pp 737 – 746), however, due to errors in data processing the constants for life prediction models published in the original paper were not accurate. These constants, along with associated figures, have been corrected here.

Figure 10: Mean Life vs. Dissipated Creep Strain Energy Density on log-log scale.

Figure 10 shows the plot of measured mean fatigue life (N_f) vs. the creep strain energy density calculated using finite element simulation on a log-log scale. The fitted model in the figure also shows the energy density exponent of -0.9229, again a value very close to theoretically derived value of –1.0 in Equation 7. This again proves the validity of the approach that the fatigue life exponent should be based on damage mechanism used to model the behavior of the material. The fitted model exponent so close to –1 again indicates that a linear regression analysis can be used for creep strain energy density based model as well.

Figure 11 shows the result of linear regression of the same data, replotted in different format (energy density vs. inverse of life), again showing a better fit than the one in Figure 9. The fitted model can be re-written in the same format as Equation 7 as

$$N_f = (0.0015\ w_{acc})^{-1} \quad (15)$$

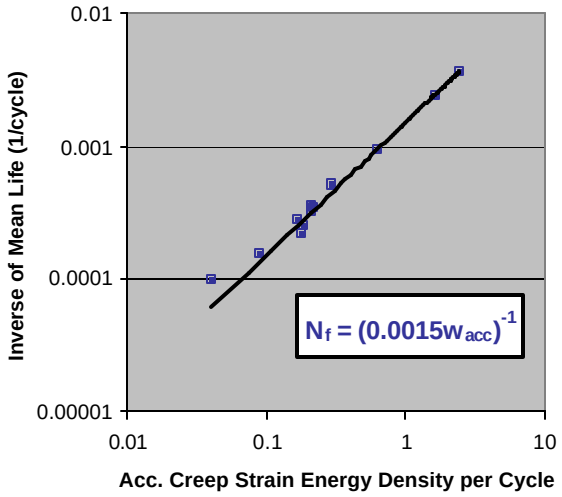

Figure 11: Inverse of Mean Life vs. Dissipated Creep Strain Energy Density on log-log scale.

Life Prediction Models for Hyperbolic Sine Constitutive Equation

The life prediction models discussed above are determined when double power law was used to simulate the creep behavior of SnAgCu solder joints. Since a number of constitutive models are proposed for SnAgCu solder, the life prediction model parameters would depend on the constitutive equation used to simulate solder behavior. In order to investigate the effect of constitutive equation, the same 12 data points for SnAgCu solder were simulated using the hyperbolic sine relationship, given by Equation 2 in Table 1.

$$\dot{e}_{cr} = A_1[\sinh(a\,s)]^n \exp\left(\frac{-H_1}{kT}\right)$$

This equation was implemented in ANSYS by using standard implicit creep equation (TBOPT = 8). The accumulated creep strain and dissipated creep strain energy density were calculated for each case and the life prediction model parameters were determined using linear regression analysis. Again a good fit was found for the data and the mean life can be predicted by using the following equations.

Acc. Creep Strain:

$$N_f = (0.0513\,e_{acc})^{-1} \quad (16)$$

Creep Energy Density:

$$N_f = (0.0019\ w_{acc})^{-1} \quad (17)$$

Comparing above to the life prediction models for double power law creep constitutive equation, the exponents are again determined as –1 for both accumulated creep strain and creep strain energy density. The values of constants, however, are slightly different. This difference is due to the actual values of creep strain and energy density calculated from two constitutive models.

This shows that the life prediction model cannot be independent of deformation constants used to simulate the material behavior. This effect will be further discussed in detail in a separate paper.

Life prediction Models Validation and Comparison

The data used in above life prediction models development encompassed different substrate types, ball count and sizes, ball pitches, material sets, die sizes, board thickness, and temperature cycle conditions.

In order to further validate the model, a completely different package was simulated and tested. The package used is PS-etCSP™ (Package Stack-extremely thin CSP), which is a stack package design. The test and simulations were conducted for single and double sided assemblies, with and without package stacking. The details of this package and test data is described elsewher e [15].

Table 3: Predicted vs. Measured life for Stack Package.

Stack	Assembly	Measured Mean Life (cycles)	Predicted Lives (cycles)			
			Power Law		Sinh	
			Acc. Creep	Energy Density	Acc. Creep	Energy Density
No	Single Sided	1225	1082	1173	995	1112
No	Double Sided	565	574	600	585	608
Yes	Single Sided	915	958	1031	904	1000
Yes	Double Sided	495	536	557	546	560

Table 3 compares the measured life with the predicted life using four life prediction models. Of the four models, the accumulated creep strain model based on power law creep equation predicted life closest to the measured data. The accumulated creep strain based on hyperbolic sine creep

A Note to reader: This paper was originally published in ECTC 2004 conference proceedings (pp 737 – 746), however, due to errors in data processing the constants for life prediction models published in the original paper were not accurate. These constants, along with associated figures, have been corrected here.

equation resulted in slightly higher predicted values. The energy density based models resulted in highest predicted values.

The same trends were observed for data in Table 2 and their respected predicted values. However, the energy density based models do seem to give the same trend as measured life when TC1 and TC2 test cycle data was compared, i.e., lower life for TC2.

Characteristic and %BX life calculations

The above life prediction models predict the mean life, not the characteristic life associated with 2 parameter Weibull distribution. The characteristic life (63.2%), however, can be easily calculated using the predicted mean life and the estimated slope (β) of Weibull distribution. This slope is typically around 10 for area array type packages, but can range between 6 and 20. In fact, the data shown in Table 2 has an average β of about 11 for both SnAgCu and SnPb solder joints. Knowing the β and the mean life, the characteristic life can be estimated using GAMMALN function in Excel spreadsheet by using the following equation

$$\text{Characteristic Life} = \text{Mean Life} / \text{EXP}(\text{GAMMALN}(1+1/\beta))$$

Using the β of 10, the above equation results in the characteristic life to be about 1.05X of mean life.

Once the characteristic life is determined, the life for any other cumulative failure rate can be determined by using 2 - parameter Weibull equation.

Summary and Conclusions

Thermal fatigue life prediction models are presented using double power law and hyperbolic sine constitutive equations for SnAgCu solder joints. Both accumulated creep strain and creep energy density approaches are used and the life prediction models are developed using damage mechanisms. The partitioning of creep strain shows that the contribution of low stress region is very small in total creep strain during an accelerated temperature cycle.

Since partitioning of creep strain is not required, the modeling approach can be easily implemented in ANSYS using standard features. The creep equations used are standard options in ANSYS and the accumulated creep strain and creep strain energy density are calculated by ANSYS directly. Post processing of results is required, however, to calculate volume averaged values in a 25 micron thick layer of solder. This can be easily accomplished using ETABLE commands in ANSYS. Although the model parameters are dependent on the finite element techniques used here, they can be used as long as 3-D modeling and volume averaging techniques are employed.

The constants of life prediction models were determined using actual test data and finite element simulations. These constants were calculated for both types of constitutive equations, showing slight difference in values.

All models show very good correlation with test data with predictions with 25% in most cases. Further validation on stacked package configuration shows life prediction approach using accumulated creep strain and double power law creep equation gives the closest results compared to experimental data.

Acknowledgments

The author would like to thank W J Kang, J Y Khim, Y J Kim, and Y H Ka at Amkor Technology, Korea for performing the reliability tests and data analysis used in this work.

References

1. Syed, A., "Reliability of Lead-Free Solder Connections for Area-Array packages," IPC SMEMA Council APEX 2001, pp. LF2-7.
2. Bartelo, J., et al, "Thermomechanical Fatigue Behavior of Selected Lead-Free Solders," IPC SMEMA Council APEX 2001, pp. LF2-2.
3. Schubert, A., et al, "Reliability Assessment of Flip-Chip Assemblies with Lead-free Solder Joints," 52nd ECTC 2002, pp. 1246-1255.
4. Syed, A. R., "Factors Affecting Creep-Fatigue Interaction in Eutectic Sn/Pb Solder Joints," Advances in Electronic Packaging 1997, InterPack97, pp. 1535-1542.
5. Syed, A., "Predicting Solder Joint Reliability for Thermal, Power, & Bend Cycle within 25% Accuracy," 51st ECTC 2001, pp. 255-263.
6. Wiese, S., et al, "Microstructural Dependendence of Constitutive Properties of Eutectic SnAg and SnAgCu Solders," 53rd ECTC 2003, pp. 197-206.
7. Schubert, A., et al, "Fatigue Life Models of SnAgCu and SnPb Solder Joints Evaluated by Experiements and Simulations," 53rd ECTC 2003, pp. 603-610.
8. Zhang, Q., et al, "Viscoplastic Constitutive Properties and Energy-Partioning Model of Lead-Free Sn3.9Ag0.6Cu Solder Alloy," 53rd ECTC 2003, pp. 1862-1868.
9. Morris, J. W., et al, "Creep Properties of Sn-rich Solder Joints, " 53rd ECTC 2003, pp. 54-57.
10. Hua, F., Private Communications
11. Wong, B., et al, "A Creep-Rupture Model for Two-Phase Eutectic Solders," IEEE CHMT-11,No.3, pp. 284-290, 1988.
12. Darveaux, R., et al, "Reliability of Plastic Ball Grid Array Assembly," Chapter 13 in Ball Grid Array Technology, Ed. Lau, J. H., McGraw-Hill, 1995.
13. Lee, W. W., et al, "Solder joint fatigue models: review and applicability to chip scale packages," Microelectronics Reliability, Vol. 40 (2000), pp. 231-244.
14. Syed, A. R., "ACES of Finite Element and Life Prediction Models for Solder Joint Reliability," Design and Reliability of SolderS and Solder Interconnections, Proceedings of Symposium 1997 TMS Conference, pp. 347-355.
15. Kim, J-Y., et al, "Board Level Reliability Study on Three-Dimensional Thin Stacked Package," to be published 54TH ECTC, 2004.

A Note to reader: This paper was originally published in ECTC 2004 conference proceedings (pp 737 – 746), however, due to errors in data processing the constants for life prediction models published in the original paper were not accurate. These constants, along with associated figures, have been corrected here.

Accumulated Creep Strain and Energy Density Based Thermal Fatigue Life Prediction Models for SnAgCu Solder Joints

Ahmer Syed

asyed@amkor.com

Presented at
54th
Electronic Components & Technology Conference
June 3, 2004

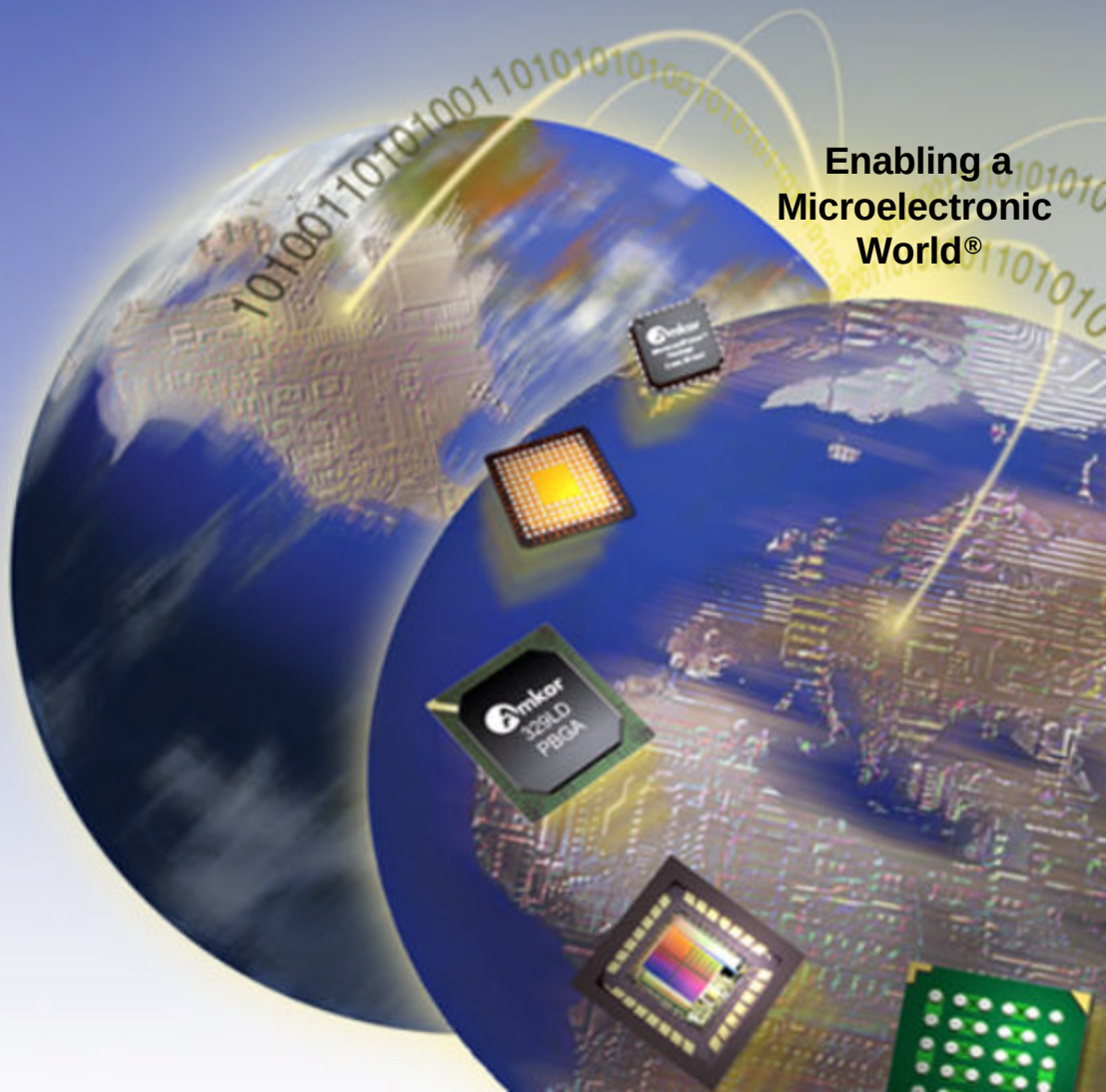

Amkor Technology

Life Prediction Models for SnAgCu Solder

- **Why Predict**
  - Industry is fast migrating to SnAgCu solder alloys
  - Reduced design cycle time limits the use of testing to evaluate reliability
  - Life prediction models are needed to assess reliability at the design stage

- **Four factors governing life prediction**
  - Material behavior
  - Simulation techniques
  - Life prediction methodology
  - Test data

1. Material Behavior

- **Constitutive equations for SnAgCu solder joints**
  - Double Power Law
    - Wiese et al (Sn4.0Ag0.5Cu)

$$\dot{e}_{cr} = A_1 \exp\left(\frac{-H_1}{kT}\right)\left(\frac{s}{s_n}\right)^{n1} + A_2 \exp\left(\frac{-H_2}{kT}\right)\left(\frac{s}{s_n}\right)^{n2}$$

A_1 = 4E-7 s^{-1}
H_1/k = 3223
n_1 = 3.0
A_2 = 1E-12 s^{-1}
H_2/k = 7348
n_2 = 12.0

    - Morris et al (Sn3.0Ag0.5Cu)

  - Hyperbolic Sine
    - Schubert et al (Sn3.8Ag0.7Cu, Sn3.5Ag0.75Cu, Sn3.5Ag0.5Cu, CASTIN™)

$$\dot{e}_{cr} = A_1[\sinh(a\,s)]^n \exp\left(\frac{-H_1}{kT}\right)$$

A_1 = 277984 s^{-1}
a = 0.02447 MPa^{-1}
n = 6.41
H_1/k = 6500

E(MPa) = 61251 – 58.5T(°K)
CTE = 20.0 ppm/K,
Poisson's ratio = 0.36

    - Zhang et al (Sn3.9Ag0.6Cu)

1. Material Behavior

- **Steady State Creep Rate Prediction**
  - SnAgCu solder is significantly more creep resistant at low stresses compared to SnPb solder
  - Similar creep behavior from 3 models at stresses below 30 MPa
    - Models diverge at high stresses

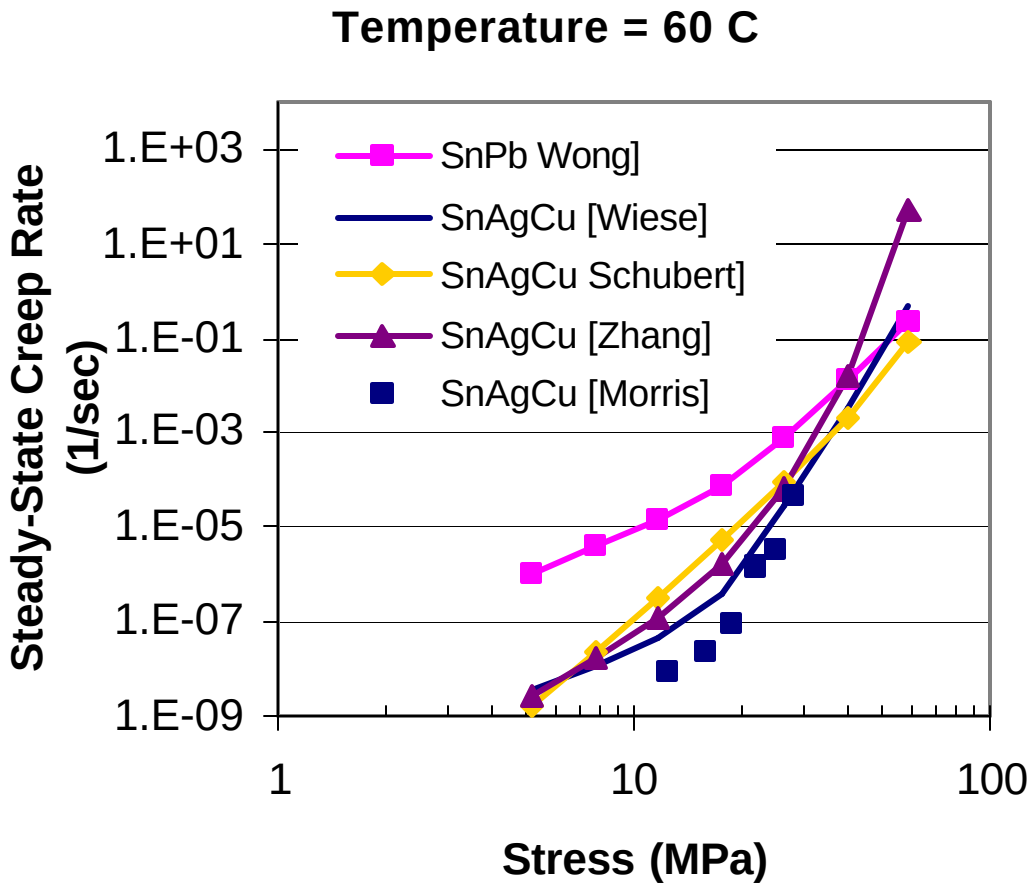

2. Finite Element Analysis

- **Same approach as SnPb solder**
  - Step 1: Build 3D Model
    - Simple representation of solder joints
    - Perform linear analysis to determine the location of critical joint
  - Step 2: Substructuring
    - Lump all elements with linear, temperature independent properties into a superelement
    - Perform superelement analysis for 1^{o}C change in temperature
  - Step 3: Build Critical Joint Model
    - Attach Superelement from Step 2
    - Model Viscoplastic and temperature dependent behavior of solder
    - Perform nonlinear analysis
- **Detailed approach in ECTC'01**

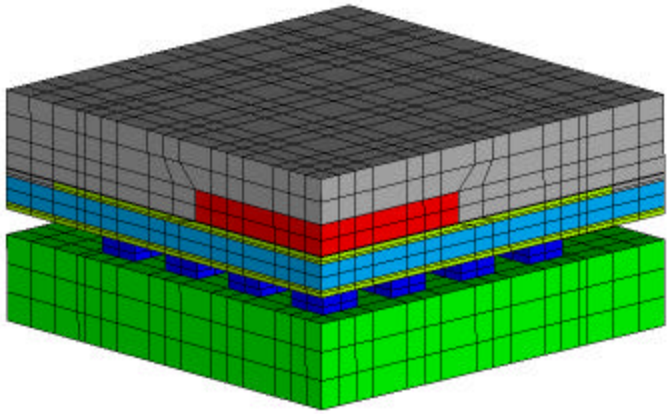

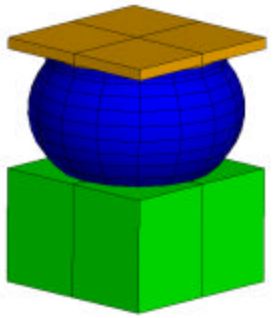

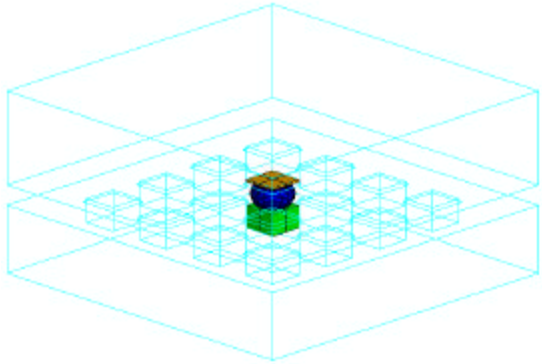

2. Finite Element Analysis

- **Solder joint response calculation**
  - Inelastic strain and energy density calculated by volume averaging
    - 25 micron thick layers of solder at package and board side
    - Each layer has two elements across the thickness
  - Life prediction model parameters are only valid for this thickness
  - Besides 3-D modeling, this is the only requirement for life prediction model
    - Substructuring only to improve efficiency

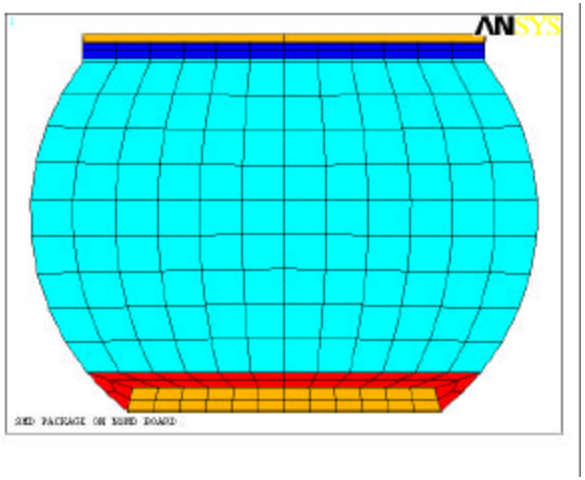

2. Solder Joint Response

- **Effect of Time Independent Plasticity**
  - Wiese's Model (Creep only VS Creep + Plasticity)
  - Ceramic BGA on FR4
  - -55 <> 125 C cycle, fast ramps (highest stress condition)

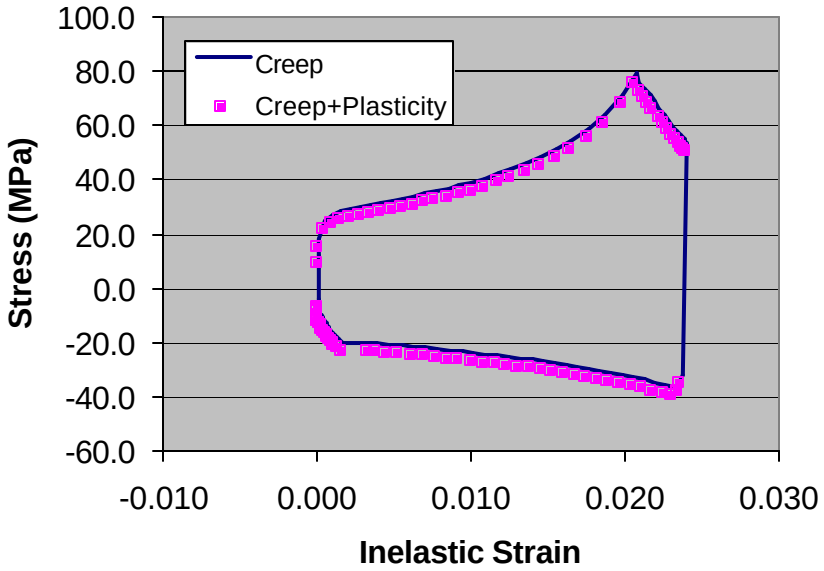

	Creep Only	Creep + Plasticity
Creep Strain %	0.4641	0.4629
Plastic Strain %	NA	0.00058
Total Strain %	0.4641	0.46348
% Plastic		**0.125**
Creep ED	1.776	1.77
Plastic ED	NA	0.004
Total Energy Density	1.776	1.774
% Plastic		**0.225**

  - Plastic strain and Energy Density contributions are insignificant in total inelastic response

- **No need to model time independent plasticity for Thermal Cycle simulations**

3. Life Prediction Model Development

- **Solder joint life is governed by Creep**
- **Thermal Cycle Fatigue ➔ Cyclic Creep Rupture**
  - Creep due to sequence of loading, repeated in a cyclic manner
  - Monkmann-Grant Equation & Time Fraction Rule

$$t_r = \frac{C}{\dot{e}_{cr}} \qquad N_f \left(\sum_{i=1}^{n} \frac{\Delta t_i}{t_{ri}} \right)_{one\ cycle} = 1$$

Dt_i = time spent at stress level s_i within a cycle, and
t_{ri} = rupture time for stress level s_i.

  - Combine

$$N_f = (C' e_{acc})^{-1} \qquad N_f = (W' w_{acc})^{-1}$$

- **For two mechanisms (double power law creep)**

$$N_f = \left(C_I e_{acc}^{I} + C_{II} e_{acc}^{II}\right)^{-1} \qquad N_f = \left(W_I w_{acc}^{I} + W_{II} w_{acc}^{II}\right)^{-1}$$

- **Constants to be determined by relating mean life (test) with solder joint response (simulations)**
- **Same approach has been successfully used for SnPb solder for 8+ years**

4. Fatigue Test Data

- **Thermal cycle tests conducted on various packages with different substrate types, body sizes, ball pitches, land sizes**

Data Point	Package Type	Substrate Type	Body Size	I/O	Pitch	Die Size	Pad Type	Pad Size	Ball Dia	Test Type	Board Thickness
1	CABGA	Laminate	15 x 15	208	0.8	8.5 x 8.5 x0.265	SMD	0.4	0.46	TC1	1.0
2	CABGA	Laminate	15 x 15	256	0.65	10 x 10 x 0.265	SMD	0.32	0.4	TC2	0.8
3	CABGA	Laminate	8 x8	64	0.8	4.8 x 4.8 x 0.29	SMD	0.4	0.46	TC1	1.6
4	CABGA	Laminate	8 x8	64	0.8	4.8 x 4.8 x 0.29	SMD	0.4	0.46	TC2	1.6
5	Ceramic BGA	Ceramic	8 x8	64	0.8	None	SMD	0.4	0.46	TC1	1.6
6	Ceramic BGA	Ceramic	8 x8	64	0.8	None	SMD	0.4	0.46	TC3	1.6
7	CVBGA	Laminate	12 x 12	288	0.5	7.1 x 7.1 x 0.175	SMD	0.25	0.3	TC1	0.8
8	fleXBGA	Tape	12 x 12	144	0.8	6.4 x 6.4 x 0.3	SMD	0.3	0.46	TC1	1.6
9	fleXBGA	Tape	12 x 12	144	0.8	6.4 x 6.4 x 0.3	SMD	0.3	0.46	TC2	1.6
10	fleXBGA	Tape	12 x 12	144	0.8	6.4 x 6.4 x 0.3	SMD	0.3	0.46	TC3	1.6
11	PBGA	Laminate	27 x 27	256	1.27	10 x 10 x 0.30	SMD	0.65	0.76	TC2	1.6
12	TSCSP	Tape	12 x 12	288	0.5	top: 5.08 x 5.08 x 0.15 btm: 10.16 x 10.16 x 0.15	SMD	0.24	0.3	TC2	0.8

- **Three test conditions**
  - TC1: -40<>125^{o}C, 15 minutes ramps and dwells, 1 cycle/hr
  - TC2: -55 <> 125^{o}C, 2 minutes ramps, 13 minutes dwells, 2 cycles/hr
  - TC3: 0 <> 100^{o}C, 10 minute ramps, 5 minutes dwells, 2 cycles/hr
- **Various board thickness'**

4. Fatigue Test Data

- **SnAgCu vs. SnPb solder measured fatigue life**

Package Attributes				SnAgCu Solder				SnPb Eutectic Solder			
Data Point	Package Type	Body Size	I/O	1st Failure	Weibull Slope	Weibull Char. Life (Cycles)	Mean Life (Cycles)	1st Failure	Weibull Slope	Weibull Char. Life (Cycles)	Mean Life (Cycles)
1	CABGA	15 x 15	208	2491	8.92	3717	3520	2539	10	3450	3281
2	CABGA	15 x 15	256	3380	15.4	4096	3960	1856	7.4	2725	2557
3	CABGA	8 x8	64	3463	8.36	4843	4570	2445	11.76	3212	3076
4	CABGA	8 x8	64	2493	9.81	3263	3103	2205	13.76	2664	2565
5	Ceramic BGA	8 x8	64	318	7.08	445	417	340	10	437	416
6	Ceramic BGA	8 x8	64	853	9.55	1103	1047	982	8.96	1316	1246
7	CVBGA	12 x 12	288	1332	5.81	2005	1890	1700	9.26	2291	2172
8	fleXBGA	12 x 12	144	2580	19.06	2948	2868	2369	10.4	3164	3015
9	fleXBGA	12 x 12	144	2351	20.4	2792	2720	1902	15.2	2410	2327
10	fleXBGA	12 x 12	144	8939	15.7	10370	10027	5042	12.95	6195	5953
11	PBGA	27 x 27	256	4651	7.2	6812	6381	3656	13.92	4544	4378
12	TSCSP	12 x 12	288	175	6	296	275	NA	NA	NA	NA

  - Life for SnAgCu solder joints is longer, but not for every case
  - Acceleration factors between test conditions are not the same

Life Prediction for SnPb Joints

$$\dot{e}_{cr} = B_I \exp\left(\frac{-H}{kT}\right)\left(\frac{s}{\mathrm{E}(T)}\right)^{n_1} + B_{II} \exp\left(\frac{-H}{kT}\right)\left(\frac{s}{\mathrm{E}(T)}\right)^{n_2}$$

$$N_f = \left(0.02 e^{I}_{acc} + 0.063 e^{II}_{acc}\right)^{-1}$$

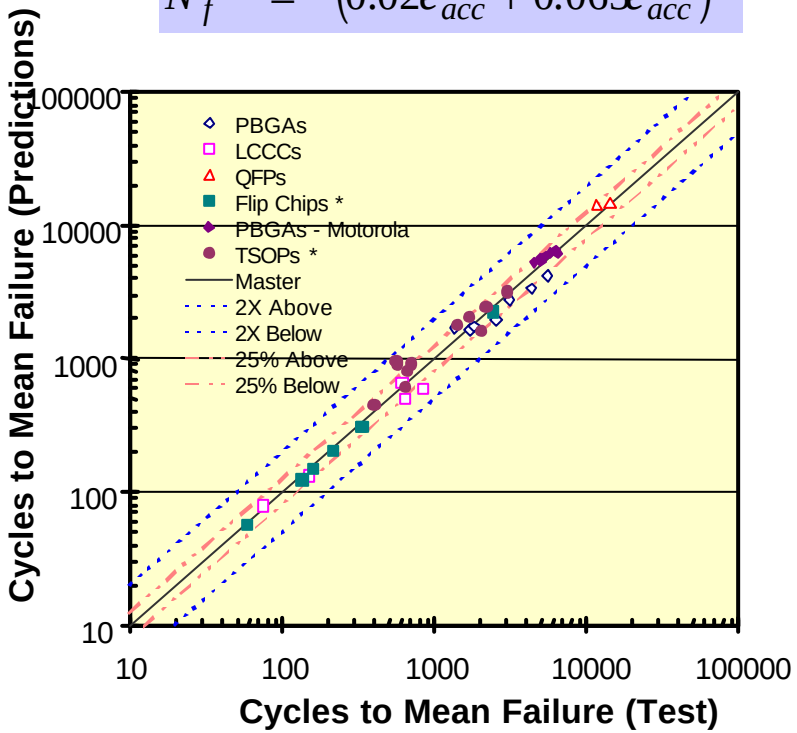

Prediction Accuracy: ± 25%

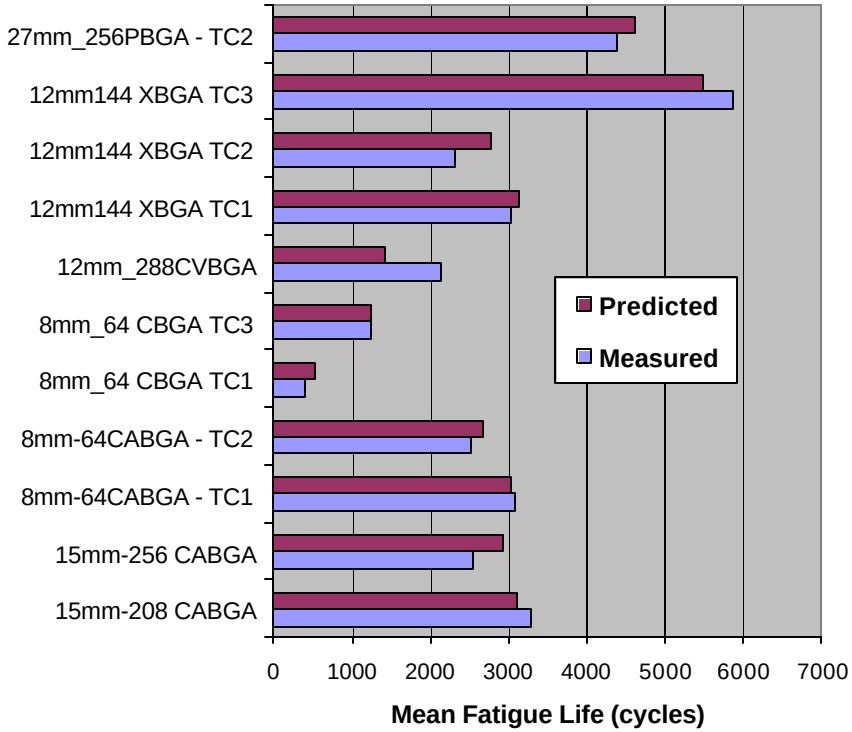

- **Provides confidence in properties used for package and board materials**
- **Failure location is correctly predicted**

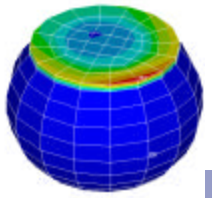

SnAgCu Solder Life Prediction

- **5 life prediction models attempted depending on the constitutive equation for SnAgCu solder**

- **Double power law creep (Wiese et al)**
  - Creep Strain Partitioning
  - Total Accumulated Creep Strain
  - Total Accumulated Creep Strain Energy Density
- **Hyperbolic sine creep (Schubert et al)**
  - Total Accumulated Creep Strain
  - Total Accumulated Creep Strain Energy Density

ANSYS Implementation

- **Creep Model Implementation in ANSYS**
  - Double Power Law Model

$$\dot{e}_{cr} = A_1 \exp\left(\frac{-H_1}{kT}\right)\left(\frac{s}{s_n}\right)^{n1} + A_2 \exp\left(\frac{-H_2}{kT}\right)\left(\frac{s}{s_n}\right)^{n2}$$

    - Standard Implicit Creep Model , TBOPT = 11 with C3 = 0.0
    - Creep strain partitioning in POST PROCESS, if needed
    - No need for USER SUBROUTINE
    - Post Processing text file can be provided.
  - Hyperbolic Sine Model

$$\dot{e}_{cr} = A_1 [\sinh(a\, s)]^n \exp\left(\frac{-H_1}{kT}\right)$$

    - Standard Implicit Creep Model , TBOPT = 8
- **Output Parameters**
    - NL, CREQ = Accumulated Creep Strain
    - SEND, CREEP = Creep Strain Energy Density

SnAgCu Solder Life Prediction

- **Cyclic stability**

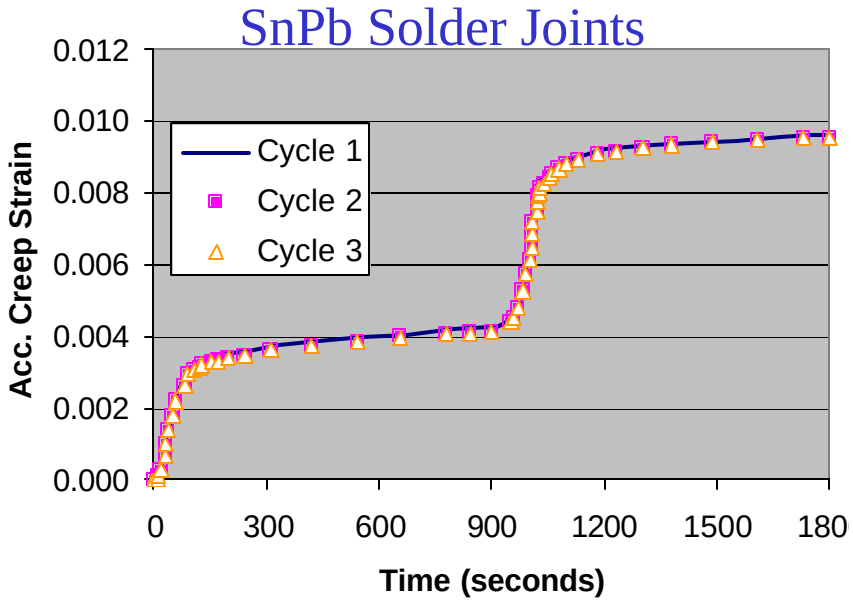

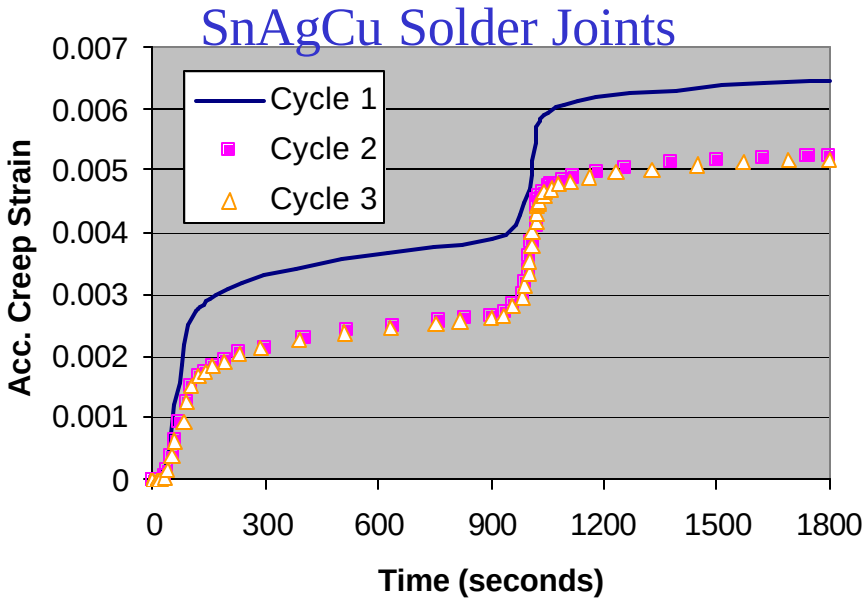

  - SnPb solder joints show cyclic stability after 1st cycle
  - SnAgCu solder joints show stability after 2nd cycles
    - 20 to 30% reduction after 1st cycle
- **Life prediction model parameters in the paper are based on 1st cycle values due to post processing error and are not correct**

SnAgCu Solder Life Prediction

$$\dot{e}_{cr} = A_1 \exp\left(\frac{-H_1}{kT}\right)\left(\frac{s}{s_n}\right)^3 + A_2 \exp\left(\frac{-H_2}{kT}\right)\left(\frac{s}{s_n}\right)^{12}$$

$$N_f = \left(C_I\, e_{acc}^{I} + C_{II}\, e_{acc}^{II}\right)^{-1}$$

- **Double Power Law Creep**
  - Creep Strain Partitioning

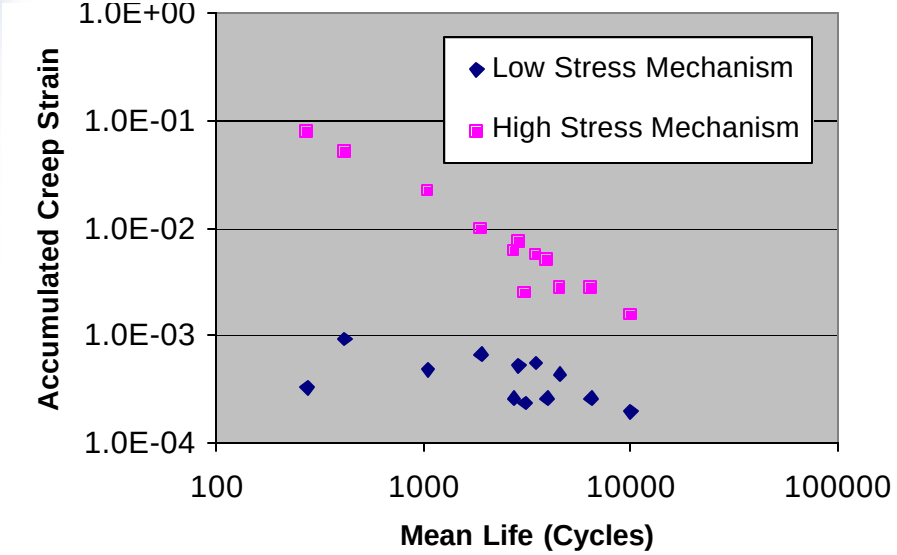

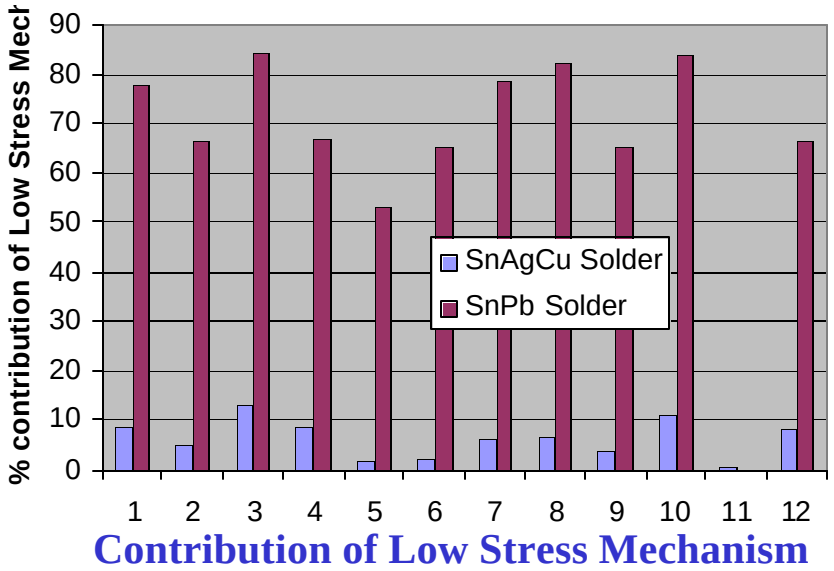

  - More scatter in low stress creep for SnAgCu solder
  - % contribution of low stress creep is < 10%
  - Significantly different response compared to SnPb Solder
- **Creep strain partitioning not needed for SnAgCu solder joints**

SnAgCu Solder Life Prediction

- **Double Power Law Creep**
  - Total accumulated creep strain & energy density approach
  - Std curve fit
    - Mean Life Vs Strain
    - Mean Life Vs Energy density
  - Curve fit for both show fatigue life exponent to be very close to 1.0

$$\dot{e}_{cr} = A_1 \exp\left(\frac{-H_1}{kT}\right)\left(\frac{s}{s_n}\right)^3 + A_2 \exp\left(\frac{-H_2}{kT}\right)\left(\frac{s}{s_n}\right)^{12}$$

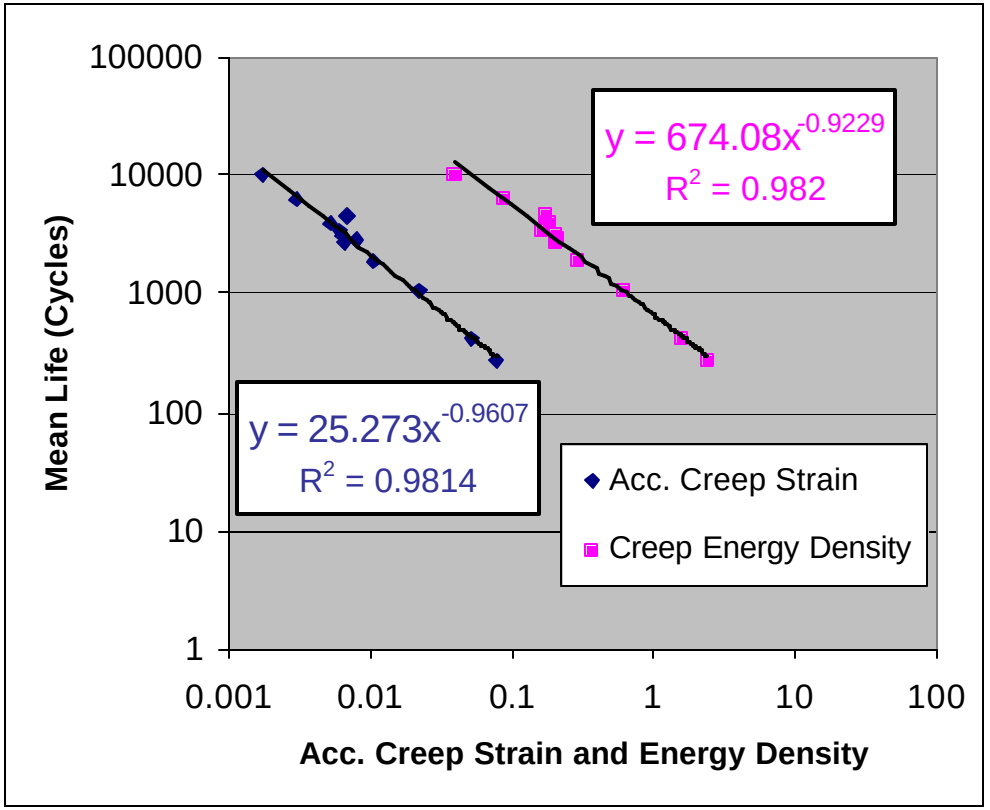

SnAgCu Solder Life Prediction

- **Double Power Law Creep**
  - Total creep and energy density

$$N_f = (C' e_{acc})^{-1}$$

$$N_f = (W' w_{acc})^{-1}$$

  - Constants determined by relating solder joint response with measured life

$$C' = 0.0468$$

$$W' = 0.0015$$

  - Acc. creep strain model seems to provide better fit at high life numbers

$$\dot{e}_{cr} = A_1 \exp\left(\frac{-H_1}{kT}\right)\left(\frac{s}{s_n}\right)^3 + A_2 \exp\left(\frac{-H_2}{kT}\right)\left(\frac{s}{s_n}\right)^{12}$$

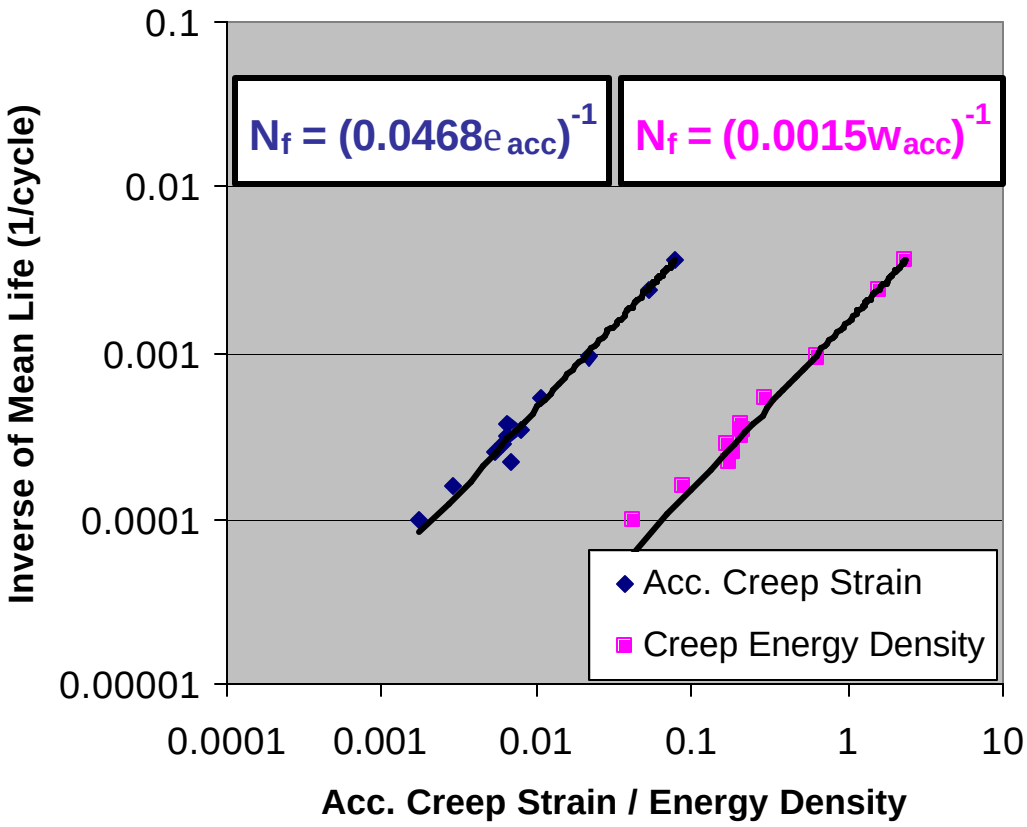

SnAgCu Solder Life Prediction

- **Hyperbolic Sine Creep**
  - Similar model but different constants

$$N_f = (0.0513 e_{acc})^{-1}$$

$$N_f = (0.0019\ w_{acc})^{-1}$$

  - Energy density based model provides better fit at higher life numbers
  - Acc. Strain based model provides conservative estimate

$$\dot{e}_{cr} = A_1[\sinh(a\,s)]^n \exp\left(\frac{-H_1}{kT}\right)$$

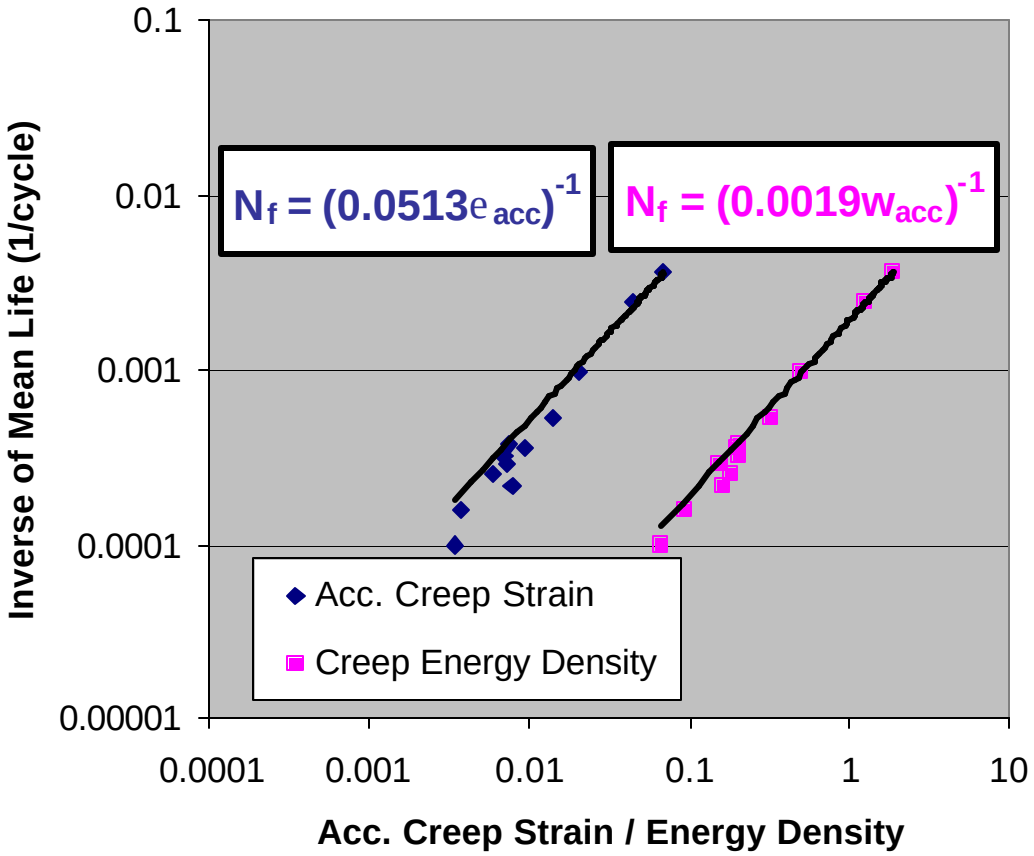

SnAgCu Solder Life Prediction

- **Which method is better?**

Package	SnAgCu Mean Life (Test)	Prediction Accuracy			
		Double Power Law		Hyperbolic Sine	
		Acc. Creep Strain	Energy Density	Acc. Creep Strain	Energy Density
15mm-208 CABGA	3519	0%	15%	-24%	-4%
15mm-256 CABGA	3960	3%	-6%	-16%	-26%
8mm-64CABGA - TC1	4570	-31%	-16%	-45%	-28%
8mm-64CABGA - TC2	3101	8%	4%	-10%	-16%
8mm-64 CBGA TC1	417	0%	0%	5%	1%
8mm-64 CBGA TC3	1047	-7%	2%	-8%	2%
12mm-288CVBGA	1890	7%	20%	-27%	-14%
12mm-144 XBGA TC1	2866	-5%	11%	-27%	-6%
12mm-144 XBGA TC2	2720	21%	18%	-5%	-6%
12mm-144 XBGA TC3	10027	22%	65%	-44%	-21%
27mm-256PBGA - TC2	6381	14%	18%	-18%	-12%
12mm-288TSCSP	275	1%	1%	1%	0%

- **Models based on Power law creep equation provide better accuracy**
  - Accumulated creep strain based model slightly better

2. Solder Joint Response

- **Creep Strain**
  - Accumulated vs. range

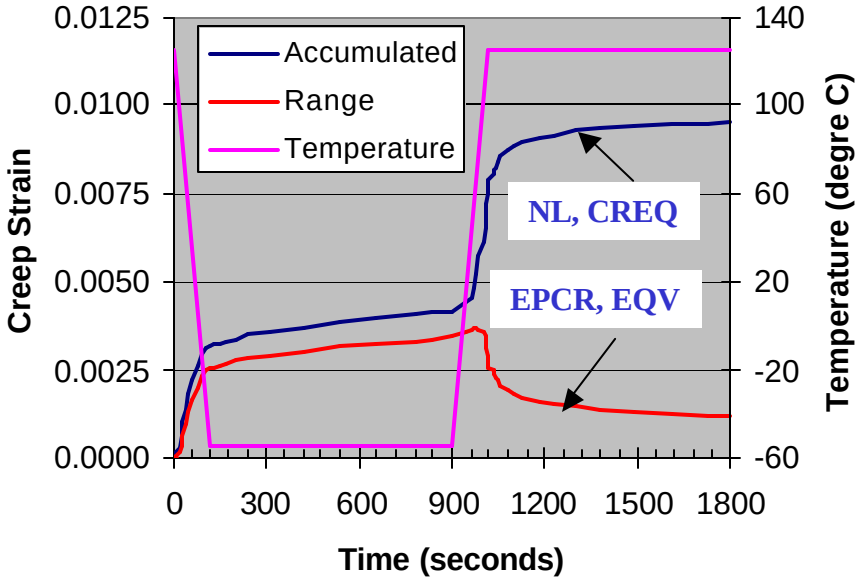

  - Most accumulation during ramps, some during dwell times at low and high temperatures

- **Strain Energy Density (Creep)**

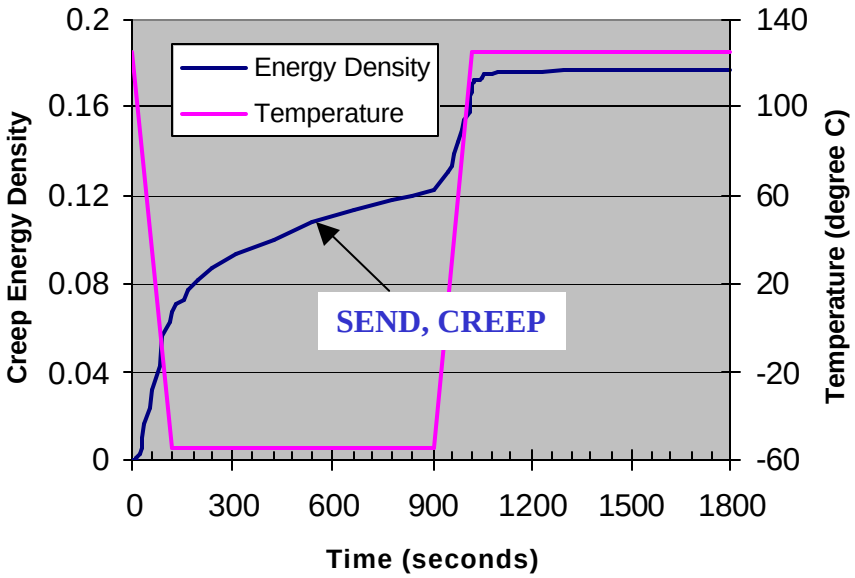

  - Significant accumulation during low temperature dwell
    - High stresses at low temp
  - Almost no accumulation during high temp dwell

SnAgCu Solder Life Prediction

- **Trend Predictions**
  - 3 test conditions, 12mm-144 fleXBGA package
  - Predictions show same trend as actual test data
  - Acceleration factors are different for SnPb and SnAgCu

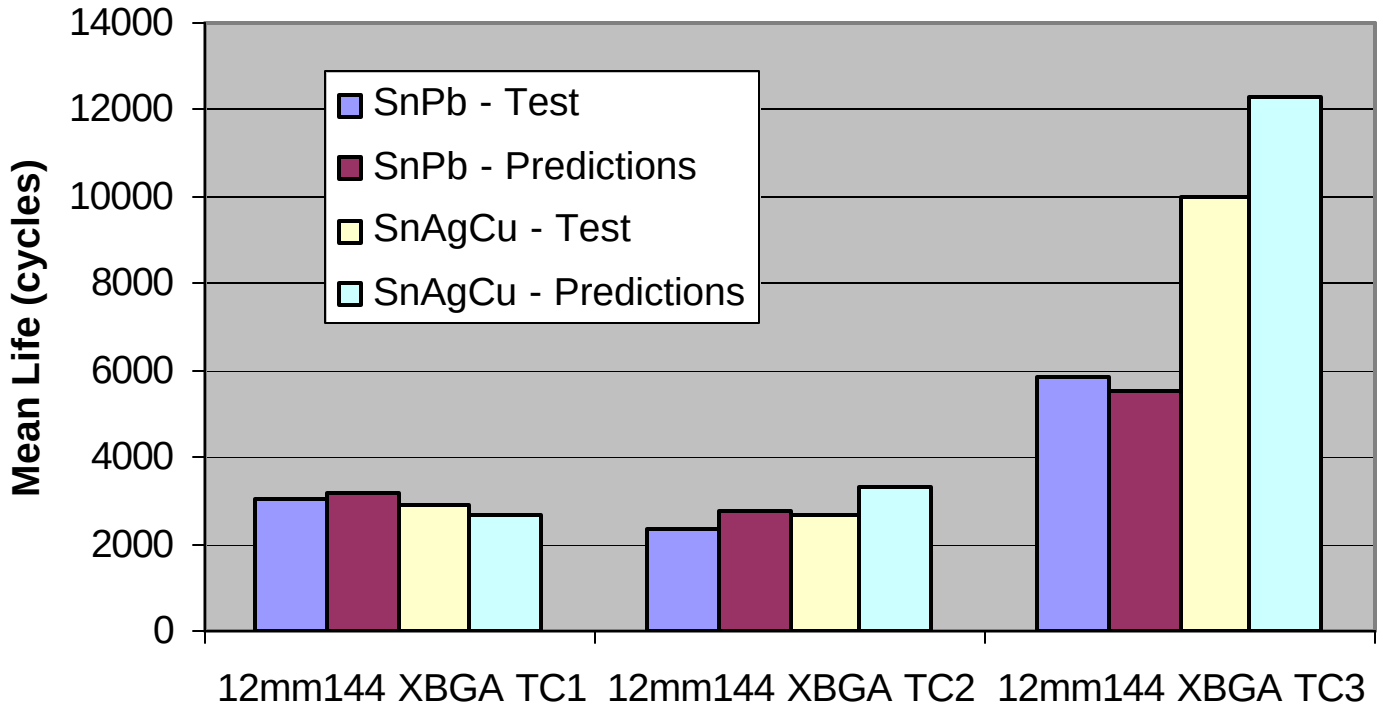

Model Validation

- **12mm-320 etCSP package – with and without stacking**
  - Single sided
  - Double sided

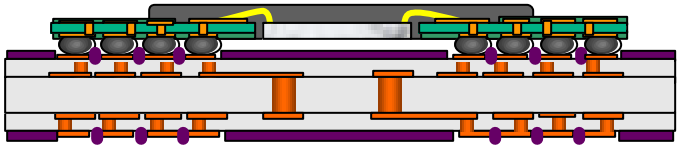

12x12mm-320 Ball etCSP

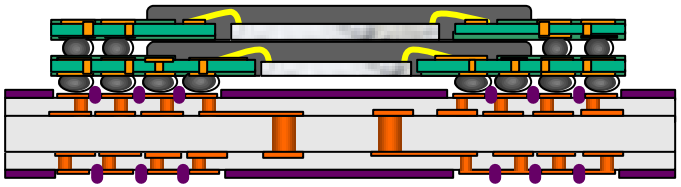

12x12mm-64 etCSP Stacked on 12x12mm-320 etCSP

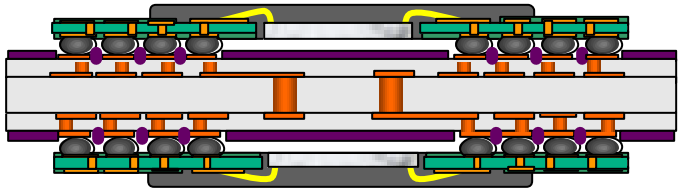

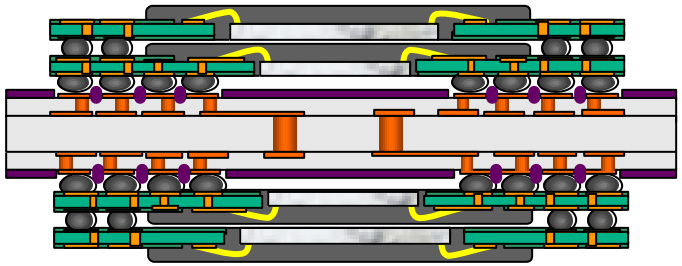

Stacked ?	Assembly	Measured Life	Predicted (Power law)		Predicted (Hyp Sine)	
			Strain	Ener Den	Strain	Ener Den
No	Single Sided	1148	1082	1173	995	1112
No	Double Sided	563	574	600	585	608
Yes	Single Sided	884	958	1031	904	1000
Yes	Double Sided	495	536	557	546	560

- **Strain based approach resulted in conservative predictions**

SnAgCu Solder Life Prediction

- **Prediction Accuracy = ±25%**
  - **18 data points**

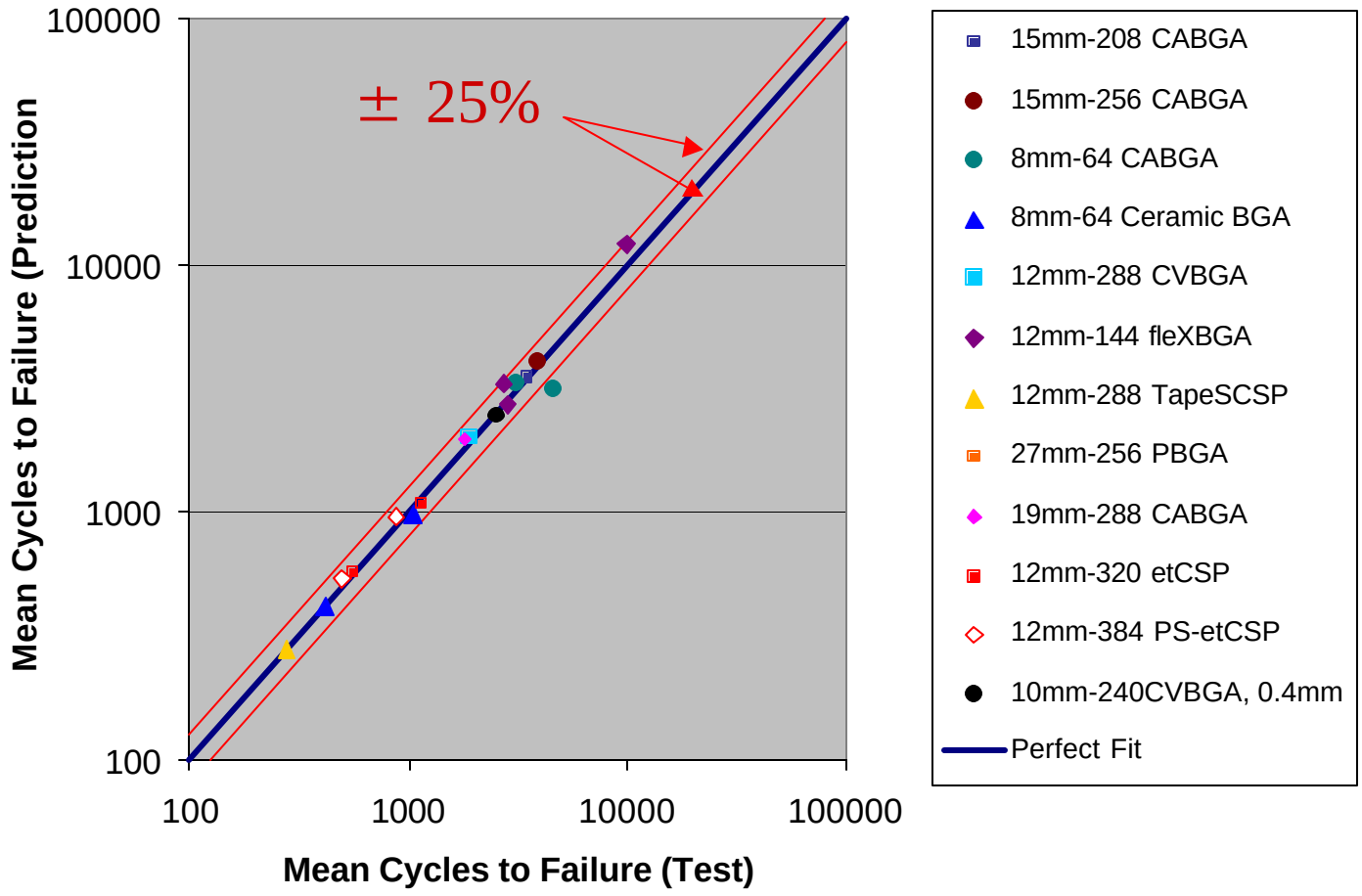

SnAgCu Solder Life Prediction

- **Conclusions**
  - Creep strain partitioning not needed for SnAgCu solder joints life prediction
  - Better prediction accuracy achieved by using double power law constitutive equation
  - Either accumulated creep strain or energy density can be used for life prediction
    - Creep strain provides better prediction accuracy
    - Energy density captures high stress effects better